Antiviral Research 91 (2011) 64–71

Contents lists available at ScienceDirect

Antiviral Research

journal homepage: www.elsevier.com/locate/antiviral

Inhibition of rabies virus propagation in mouse neuroblastoma cells by an intrabody against the viral phosphoprotein

Yoshihiro Kaku *, Akira Noguchi, Kozue Hotta, Akio Yamada, Satoshi Inoue

Department of Veterinary Science, National Institute of Infectious Diseases, 1-23-1, Toyama, Shinjuku, Tokyo 162-8640, Japan

ARTICLE INFO

Article history:
Received 2 March 2011
Revised 13 April 2011
Accepted 27 April 2011
Available online 5 May 2011

Keywords:
Rabies
Phosphoprotein
Intrabody
scFv
Intracellular immunization

ABSTRACT

Rabies virus (RABV) is highly neurotropic and causes acute infection of the central nervous system. Death can be averted by prompt post-exposure prophylaxis; however, after clinical symptoms appear, the mortality rate is almost 100% and no reliable treatment is available. In this study, we investigated whether intracellular immunization using single-chain variable fragments (scFvs) against RABV phosphoprotein (RABV-P) could inhibit RABV propagation in neuronal cells. Of four scFv clones derived from an scFv phage-displayed library, scFv-P19 showed extremely high transfection efficiency and stable expression in mouse neuroblastoma (MNA) cells. The intracellular affinity and inhibition of RABV propagation were investigated using RABV-infected MNA cells pretransfected with the scFv-P19 gene. The specific interaction between scFv and RABV-P was confirmed by an immunoprecipitation assay and an indirect immunofluorescence assay showing that these molecules colocalized in the cytoplasm. Measurements of the spread of RABV in a culture well and the virus titer in the supernatant showed that RABV inhibition peaked 3 days after infection, at 98.6% and 99.9% inhibition, respectively. Although the mechanism of RABV inhibition by scFv-P19 is not clear, this scFv-based intracellular immunization could be a candidate for future RABV therapeutic studies if combined with appropriate delivery and application systems.

1. Introduction

Rabies virus (RABV) is a highly neurotropic virus that causes an acute infection of the central nervous system (CNS). RABV inoculated into peripheral tissues is hypothesized to enter nerve terminals either after replication in the peripheral skeletal muscle or directly, without prior replication (reviewed by Schnell et al. (2010)). The virus then travels via retrograde fast axonal transport within axons in peripheral nerves, through the spinal cord and dorsal root ganglia, to brain neurons. Following the invasion of the CNS, the virus rapidly disseminates within the CNS and spreads centrifugally to peripheral sites, including salivary glands, along neuronal routes, which can result in death. Transmission to and excretion from the salivary gland is essential for transmission of RABV to its next host. Death can be averted by prompt post-exposure prophylaxis (PEP). However, if PEP is delayed and clinical symptoms develop, the mortality rate is almost 100%. So far, only a few people have been reported to have survived after the onset of clinical disease (reviewed by Nigg and Walker (2009)). In 2004, it was reported that a patient had survived rabies encephalitis without PEP, after treatment including induction of coma and administration of an antiviral drug (Willoughby et al., 2005). Several laboratories have repeated this treatment program (reviewed by Nigg and Walker (2009)); however, few successful cases have been reported (Hemachudha et al., 2006) and the efficacy of this method is still controversial. To establish more stable and successful therapy, novel neuroprotective approaches based on specific anti-RABV agents are required.

Intracellular immunization (Baltimore, 1988) is a promising therapeutic technique that uses various forms of gene transfer to provide specific cellular resistance to viral infection. One approach is the degradation of viral messenger RNA by gene silencing mediated by antisense oligonucleotides (Stein et al., 2010), ribozymes (Nawtaisong et al., 2009), or RNA interference (RNAi; Dykxhoorn et al., 2003). Another approach is the inhibition of viral protein functions or interactions by intracellularly expressed antibodies, known as intrabodies (Marasco, 1997). Each approach has advantages for therapeutic application (Cao and Heng, 2005). Intrabodies have much higher specificity against target proteins than RNAi and far longer half-lives can be attained; however, intrabodies are more time-consuming and labor-intensive to generate. The most-explored form of intrabody is the single chain variable fragment (scFv), which consists of the VH and VL regions of the variable antigen-binding site of an immunoglobulin, connected with a short linker sequence. The scFvs possess several advantages over immunoglobulins as an intrabody format: a simple and compact structure, higher stability, and increased solubility. Intrabodies

* Corresponding author. Tel.: +81 3 5285 1111; fax: +81 3 5285 1179.
E-mail address: ykaku@nih.go.jp (Y. Kaku).

0166-3542/$ - see front matter © 2011 Elsevier B.V. All rights reserved.
doi:10.1016/j.antiviral.2011.04.016

based on scFvs have been developed against human immunodeficiency virus-1 (Goncalves et al., 2002), hepatitis B virus (Yamamoto et al., 1999), hepatitis C virus (Karthe et al., 2008), rotavirus (Vascotto et al., 2004), herpes virus (Corte-Real et al., 2005), and flavivirus (Jiang et al., 1995). The intrabody-based strategy could be applied to the development of future therapeutic agents against rabies, because RABVs transfer exclusively cell-to-cell and possess highly distinct neurotropism.

In this study, we developed several scFv-based intrabodies against RABV phosphoprotein (RABV-P). RABV-P was chosen as a target for intracellular immunization because it is involved in multiple functions through interactions with various viral or cellular proteins, such as encapsidation of viral genome RNA (Chenik et al., 1994), acting as a cofactor for RABV large protein (RABV-L, a viral RNA polymerase; Chenik et al., 1998), and inhibition of the cellular antiviral system induced by interferons (Vidy et al., 2007). Using a phage-displayed scFv library, we obtained four genetically independent scFv clones. One of these scFvs, when expressed transiently in mouse neuronal cell lines before RABV infection, severely inhibited the propagation and secretion of RABV and the spread of infection. This approach could be a prospective candidate for the establishment of novel therapeutic agents against RABV infection.

2. Materials and methods

2.1. Virus and viral protein

The fixed RABV strain CVS-11 was used in this study. The recombinant RABV-P protein was prepared as described previously (Motoi et al., 2005).

2.2. Selection of scFvs against RABV-P

Human single-fold scFv libraries I + J (Tomlinson I + J; a kind gift from MRC Centre for Protein Engineering, Cambridge, United Kingdom) underwent selection for the ability to bind RABV-P protein. The libraries are based on a single human framework for VH (V3-23/DP-47 and J_H4b) and Vκ (O12/O2/DPK9 and Jκ1) with side chain diversity incorporated at positions in the antigen binding site. In the libraries, the scFv genes were linked to a His-tag followed by a myc-tag and cloned into pIT2 phagemid vectors. The selection or "panning" process was essentially as described by the manufacturer's protocol (http://www.geneservice.co.uk/products/proteomic/datasheets/tomlinsonIJ.pdf). Briefly, Nunc immunotubes (Thermo Fisher, Wiesbaden, Germany) were coated with 100 μg/mL of RABV-P in PBS. After washes with PBS and blocking with PBS containing 2% skim milk, tubes were loaded with 10^{12}–10^{13} phages and incubated for 2 h. After intensive washes, bound phages were eluted by adding 500 μL of trypsin–PBS (2 mg/mL trypsin in PBS). The eluted phages were propagated and amplified in *Escherichia coli* TG1. After three rounds of panning, individual clones were grown in a 96-well U-bottom plate. Phages were produced by adding KM13 helper phages, and the binding to RABV-P by the monoclonal phages was confirmed by enzyme-linked immunosorbent assay (ELISA). As a negative control, scFvs against an unrelated protein, immunoglobulin G (IgG) of the fruit bat *Rousettus aegyptiacus* (a kind gift from Dr. T. Omatsu, Tokyo University) were selected following the same procedure.

2.3. ELISA

The ELISA plate was coated with either native RABV-P (2 μg/well) or denatured RABV-P (2 μg/well); the latter was generated by boiling RABV-P in 2% SDS for 5 min. Nonspecific binding was blocked by PBS containing 5% skim milk. The phages (diluted 1:10) or soluble scFvs (in *E. coli* HB2151 supernatant, diluted 1:10) were added to a set of two wells (native RABV-P and denatured RABV-P antigens) and incubated for 1 h at room temperature. After the plates had been washed, the bound phages were visualized by the addition of horseradish peroxidase (HRP)-conjugated protein L (Pierce, Rockford, IL, USA) and SureBlue TMB 1-component Microwell Peroxidase Substrate (KPL, Gaithersburg, MD, USA). The optical density (OD) was read at 450 nm using a Model 680 Microplate Reader (Bio-Rad, Hercules, CA, USA).

2.4. Phagemid DNA sequencing

The phagemid vector pIT2 was isolated using a Qiagen Plasmid Midi Kit (Qiagen, Venlo, Netherlands). The phagemids were sequenced using the Big Dye Terminator v3.1 Cycle Sequencing Kit (Applied Biosystems, Foster City, CA, USA) with the 373 DNA Sequencer (Applied Biosystems). The primers used to sequence the scFv inserts in the pIT2 vector were LMB3 (5′-CAGGAAACAGCTATGAC-3′) and pHEN (5′-CTATGCGGCCCCATTCA-3′). Deduced amino acid sequences of each α-RABV-P scFv were aligned using GENETYX Ver. 9 (Genetyx, Tokyo, Japan).

2.5. Expression and purification of soluble scFvs

RABV-P-reactive and genetically independent phage clones were selected for induction of soluble scFv production. *E. coli* HB2151 was transformed with phages and inoculated in 2× TY (tryptone–yeast) medium containing 100 μg/mL ampicillin and 0.1% glucose, then grown at 37 °C until the OD_{600} reached approximately 0.5. To induce the expression of soluble scFv, 1 mM isopropyl-β-D-thiogalactapyranoside was added to the culture. After incubation for 4 h at 30 °C, the culture was centrifuged at 2600 *g* for 20 min, and the pellet was resuspended in lysis buffer (50 mM NaH_2PO_4, 300 mM NaCl, and 10 mM imidazole) and incubated on ice for 30 min. After the lysate was divided into aliquots in 2.0-mL tubes, glass beads (Sigma, St. Louis, MO, USA) were added, and the cells were disrupted with a Fast Prep Cell Disrupter (Qbiogene, Carlsbad, CA, USA) at speed 4 for 20 s. Following incubation on ice for 10 min and centrifugation at 12,000*g* for 5 min, the supernatant containing scFv and other *E. coli*-derived proteins was collected. For the purification of scFv, Ni–NTA nickel-charged resin (Qiagen) was added to the supernatant, and the mixture was rotated at 4 °C for 1 h. After centrifugation at 1000 *g* for 10 min, the pelleted Ni–NTA was washed three times with wash buffer (50 mM NaH_2PO_4, 300 mM NaCl, and 20 mM imidazole). Finally, scFv was eluted using elution buffer (50 mM NaH_2PO_4, 300 mM NaCl, and 250 mM imidazole).

2.6. Immunoprecipitation

To examine the interaction between scFv and RABV-P *in vitro*, immunoprecipitation of *E. coli*-expressed soluble scFv against RABV-P was performed using magnetic beads (Dynabeads His-Tag Isolation & Pulldown; Invitrogen, Carlsbad, CA, USA). Briefly, mouse neuroblastoma (MNA) cells were grown as a monolayer in 6-well plates, infected with RABV at a multiplicity of infection (m.o.i.) of 10, and subsequently incubated in a 5% CO_2 incubator. After 48 h, the cells were lysed with 0.5 mL of lysis buffer (50 mM sodium phosphate [pH 8.0], 300 mM NaCl, 0.01% [vol/vol] Tween-20, 1% [vol/vol] Triton-X 100) at 4 °C for 1 h. The cell lysates were centrifuged at 20,000*g* for 30 min at 4 °C. The supernatants were collected, and 2.5 μg of scFvs were added and reacted for 1 h at 4 °C. The samples were mixed with Dynabeads and incubated for 10 min, washed four times with wash buffer (50 mM sodium phosphate [pH 8.0], 300 mM NaCl, 0.01% [vol/vol] Tween-20), and then

resuspended in 20 μL loading buffer (containing 4× NuPAGE LDS Sample Buffer [Invitrogen, Carlsbad, CA, USA], 10× NuPAGE Reducing Agent [Invitrogen]). After heating the sample for 10 min at 70 °C, the samples were subjected to SDS–polyacrylamide gel electrophoresis (PAGE).

To confirm the *in vivo* interaction between the intrabody and RABV-P, immunoprecipitation was performed using a Dynabeads Protein G Immunoprecipitation Kit (Invitrogen) and lysates of scFv-transfected MNA cells with or without RABV infection. To make the cell lysates, scFv-P19-pCAG was first transfected into MNA cells as described below (see Section 2.10). After 24 h, the cells were infected with CVS-11 (m.o.i. = 10) or mock-infected. At 48 h after infection, the cells were lysed, centrifuged, and collected as described above. The manufacturer's immunoprecipitation protocol was followed, using the buffer set included in the Kit. Briefly, 1.5 mg of Dynabeads were mixed with 2.0 μg of an anti-myc tag mouse monoclonal antibody (MoAb; MBL, Nagoya, Japan) and reacted for 10 min at room temperature. After washes with Ab Binding & Washing Buffer, the cell lysates were added and reacted for 10 min. After washes with Washing Buffer, the samples were suspended in a mixture of 20 μL Elution Buffer and 10 μL loading buffer. The samples were eluted by heating for 10 min at 70 °C, and were subjected to SDS–PAGE.

2.7. SDS–PAGE and Western blotting

The precipitated proteins were suspended in loading buffer and separated by electrophoresis in NuPAGE Novex Bis–Tris Mini Gels (Invitrogen) using MES Buffer (Invitrogen). In the upper buffer chamber, NuPAGE Antioxidant (Invitrogen) was added at a concentration of 0.25%. After SDS–PAGE, the proteins were transferred onto PVDF membranes using a semidry transblotter (Bio-Rad). The membranes were blocked for 1 h at room temperature (or overnight at 4 °C) with 5% skim milk (wt/vol) in PBS.

To detect RABV-P, a rabbit anti-RABV-P polyclonal antibody, obtained by DNA immunization, was diluted 1:5000 with 1% skim milk in PBS containing 0.05% (vol/vol) Tween-20 (PBS-T) and incubated with the membranes for 1 h at room temperature. Following four washes with PBS-T, an HRP-conjugated anti-rabbit IgG, diluted 1:5000 with 1% skim milk in PBS-T, was added and incubated for 1 h at room temperature. After four washes, the membranes were developed with ECL Plus Western Blotting Detection Reagent substrate solution (GE Healthcare). The signals were detected using VersaDoc (Bio-Rad).

To detect scFvs, an anti-myc tag mouse MoAb; was added to the primary antibody solution (above) at 0.5 μg/100 μL, and HRP-conjugated goat anti-mouse IgG (H + L) (Pierce) was added to the secondary antibody solution (above) at 1:5000.

2.8. Characterization of scFv affinity

To characterize the affinity of each scFv, ELISA against immobilized RABV-P was performed using peroxidase-labeled scFvs. First, 200 μg of each soluble scFv was peroxidase-labeled using a Peroxidase Labeling Kit-NH_2 (Dojindo, Kumamoto, Japan) in accordance with the manufacturer's instructions. After the labeling, serially diluted scFvs were applied to an ELISA plate coated with native RABV-P and detected as described above (see Section 2.3). The OD data was graphed by using Prism 5 (GraphPad, San Diego, CA, USA).

2.9. scFv vectors for intrabody expression

Each scFv gene cDNA was recovered from its pIT2 phagemid vector by PCR (primer sequences will be supplied on request). For intrabody expression, each scFv gene cDNA was inserted into pCAGGS-derived pCAGJ12bsr (Kojima et al., 2003; a kind gift from Dr. Asato Kojima, National Institute of Infectious Diseases, Japan), after the removal of the original insert, J12. The generated vectors were named scFv-P19-pCAG, scFv-P38-pCAG, scFv-P80-pCAG, scFv-P115-pCAG, and scFv-bat-IgG-pCAG (negative control).

2.10. Transfection and confirmation of intrabody expression

Each intrabody expression vector was transfected into MNA cells using Fugene HD (Roche) in accordance with the manufacturer's protocol. At 1–4 days after transfection, intrabody expression was confirmed with an indirect immunofluorescence assay (IFA). Briefly, after cell fixation in 3.6% formaldehyde and 0.4% Triton-X for 30 min at room temperature, the intrabody was stained using the anti-myc tag mouse MoAb as the primary antibody and an FITC-goat anti-mouse IgG (H + L) (Invitrogen) as the secondary antibody, then viewed under a fluorescence microscope (Nikon, Tokyo, Japan). For counterstaining, 0.002% Evans blue was added to the secondary antibody fluid.

2.11. Confirmation of the interaction between the intrabody and RABV-P in vivo

scFv-P19-pCAG was transfected into MNA cells as described above. After 24 h, the cells were infected with CVS-11 (m.o.i. = 10). At 24 h after infection, the cells were fixed in 3.6% formaldehyde and 0.4% Triton-X. The intrabody was stained as described above, and RABV-P was stained with rabbit anti-RABV-P serum as the primary antibody and TRITC-conjugated anti-rabbit IgG (Sigma) as the secondary antibody. Cells were visualized and the images were digitally captured by a BZ-8000 "Bio-zero" fluorescence microscope (KEYENCE, Osaka, Japan). At 24 h after transfection, the cells were lysed and collected, and then immunoprecipitated as described above.

2.12. Measurement of inhibition of RABV propagation by the intrabody

scFv-P19-pCAG was transfected into MNA cells in a 96-well plate as above. After 24 h, the cells were infected with CVS-11 (m.o.i. = 0.005). At 1 to 4 days after infection, inhibition of RABV propagation by the intrabody was measured by two methods: (i) measurement of the proportion of an area infected with RABV, and (ii) virus titration of the supernatant. To measure the infected area, the cells were stained with FITC Anti-Rabies Monoclonal Globulin (Fujirebio Diagnostics, Malvern, PA, USA), which targets RABV nucleoprotein (RABV-N). Images of RABV-infected (RABV-N-positive) cells were captured digitally as described above. In the digital image, the proportion of the fluorescence-emitting area relative to the whole well was calculated by using VH-H1A5 "VH analyzer" software (KEYENCE), then the data were graphed by using Prism 5. To measure the viral titer, the supernatant was collected, diluted 10-fold serially, and inoculated into MNA cells. After 48 h, the cells were stained by FITC Anti-Rabies Monoclonal Globulin and titrated by the Reed & Muench method (Reed and Muench, 1938).

3. Results

3.1. Selection of scFv clones against RABV-P

After three rounds of panning, a total of 192 phage clones were obtained. The binding ability of these phage clones was examined by ELISA against native RABV-P and denatured RABV-P, and 10 clones that showed equivalent reactivity for both native and denatured RABV-P were selected. DNA sequencing of scFv cDNA in each

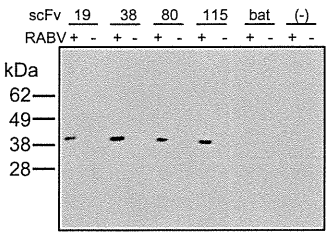

Fig. 1. *In vitro* interaction between scFvs and RABV-P confirmed by immunoprecipitation and Western blotting assays. Western blot analysis of lysates of RABV-infected and mock-infected MNA cells. The lysates were mixed with each scFv (scFv-P19, -38, -80, -115, -bat-IgG) or no scFv and immunoprecipitated with Dynabeads, blotted, and detected with a rabbit anti-RABV-P polyclonal antibody and HRP-conjugated anti-rabbit IgG.

of the 10 clones indicated that these clones converged to four genetically independent clones (Supplemental Fig. 1). *E. coli* HB2151 cells were infected with these phages to obtain soluble scFv for further characterization. After the purification of soluble scFvs using Ni–NTA resin, SDS–PAGE was performed to confirm the expression of scFvs. All four scFv clones showed a single protein band with a molecular weight of 29 kDa by SDS–PAGE (Supplemental Fig. 2). These scFvs were also confirmed to detect RABV-P by reducing Western blot analysis (data not shown), indicating that all four scFvs recognize linear epitopes.

We further performed an immunoprecipitation assay to examine the interaction *in vitro* between these scFvs and RABV-P. RABV-infected MNA cells were lysed 48 h after infection and incubated with each scFv. The protein mixture was precipitated by using magnetic beads to bind the histidine-tagged proteins. A distinct interaction between the scFvs and RABV-P was detected in a Western blot analysis with anti-RABV-P serum (Fig. 1) and the anti-myc MoAb (data not shown). To characterize the affinity of each scFv, we performed ELISA against immobilized RABV-P using peroxidase-labeled scFvs. According to the reaction curves (Supplemental Fig. 3), the affinity against RABV-P was highest in scFv-P19, followed by -115, -38, and -80.

3.2. Confirmation of intrabody expression

The scFv cDNAs of all four clones were inserted into pCAGGS-derived vectors to achieve intracellular expression as intrabodies. The generated intrabody expression vectors, scFv-P19-pCAG, scFv-P38-pCAG, scFv-P80-pCAG, and scFv-P115-pCAG, were transfected into MNA cells for transient expression, and their expression levels were monitored by IFA using an anti-myc tag MoAb. The transfection efficiency of the clones varied: scFv-P19 showed much higher transfection efficiency than the others, reaching more than 80% (estimated by eye; Fig. 2, top). Interestingly, all the scFv clones, but especially scFv-P19, showed highly stable expression without substantial diminution from 24 h until 96 h after transfection (Fig. 2). Considering its high transfection efficiency and stable expression, we selected scFv-P19 for further studies to examine *in vivo* binding with RABV-P and the ability to abrogate viral propagation.

3.3. Confirmation of the interaction between intrabodies and RABV-P in vivo

To examine the interaction between the scFv-P19 intrabody and RABV-P *in vivo*, MNA cells were transfected with scFv-P19-pCAG for transient expression, and 24 h later, the same cells were infected with CVS-11 (m.o.i. = 10). At 48 h after infection, intracellular localization of scFvs and RABV-P was observed by IFA using the anti-myc tag MoAb and anti-RABV-P polyclonal serum and compared with the localization in mock-infected MNA cells expressing scFv-P19. In mock-infected MNA cells, scFvs were located diffusely throughout the cytoplasm (Fig. 3A) without any particular condensation of fluorescence. In contrast, in CVS-11-infected MNA cells, some cells showed punctate fluorescent patterns against the background of diffuse fluorescence in the cytoplasm (Fig. 3B). We also observed this punctate fluorescence in CVS-11-infected cells stained with anti-RABV-P polyclonal serum (Fig. 3C), which is typically seen in cells infected with fixed RABV strains in culture and reportedly involves the intracellular accumulation of ribonucleoprotein complex to form Negri bodies (Lahaye et al., 2009). These punctate fluorescent patterns of scFv-P19 and RABV-P overlapped

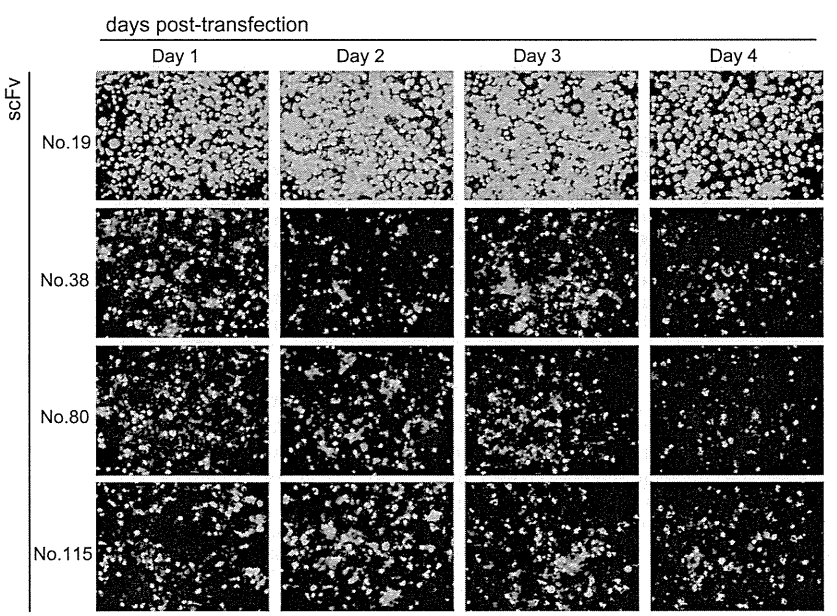

Fig. 2. Time course of intracellular expression of scFvs. In MNA cells transfected with the indicated scFv vectors, scFv was detected by a mouse anti-myc tag MoAb and FITC-conjugated anti-mouse IgG on days 1–4 after transfection. For counterstaining, 0.002% Evans blue was added to the secondary antibody fluid.

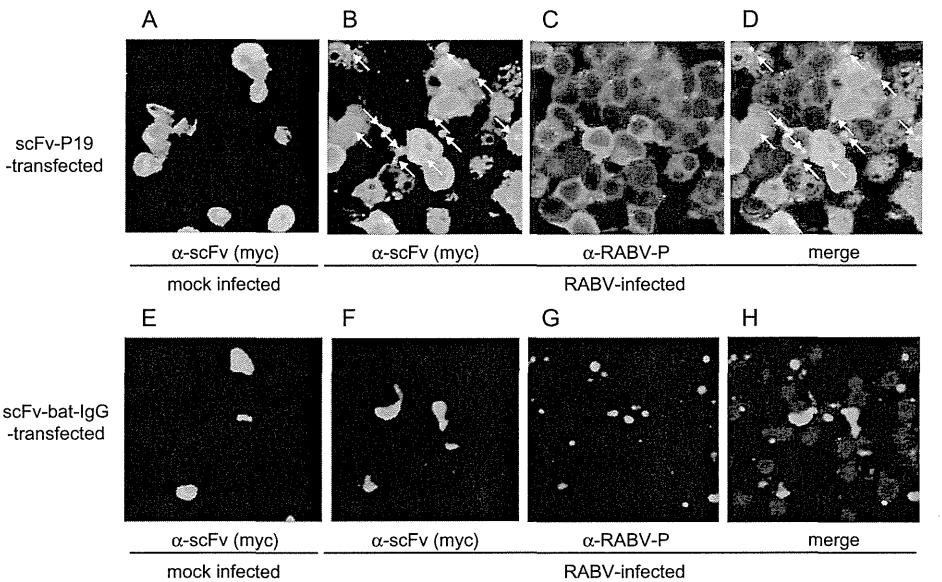

Fig. 3. Intracellular colocalization of scFv-P19 and RABV-P. MNA cells were pre-transfected with scFv-P19-pCAG (A–D) or scFv-bat-IgG-pCAG (E–H). In mock-infected MNA cells pre-transfected with scFv-expressing plasmids (A and E), scFv was detected with an anti-myc tag MoAb and FITC-conjugated anti-mouse IgG. In RABV-infected MNA cells pre-transfected with scFv-expressing plasmids, scFv was detected as described above (B and F) and RABV-P was detected with a rabbit anti-RABV-P polyclonal antibody and TRITC-conjugated anti-rabbit IgG (C and G). (D and H) Merged images of (B) and (C), or (F) and (G). Arrows in (B) and (D) indicate the punctate fluorescence of scFvs.

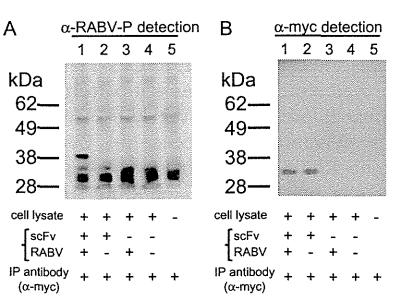

Fig. 4. *In vivo* interaction between scFv-P19 and RABV-P confirmed by immunoprecipitation and Western blotting assays. Western blot analysis of lysates of RABV-infected and mock-infected MNA cells transiently expressing scFv-P19. For detecting RABV-P (A), the lysates were immunoprecipitated (IP) with an anti-myc-tag MoAb, and the immunoblot was probed with a rabbit anti-RABV-P polyclonal antibody and detected by HRP-conjugated anti-rabbit IgG. For detecting scFv-P19 (B), the lysates were IP as above, and the immunoblot was probed with a mouse anti-myc tag MoAb and detected by HRP-conjugated anti-mouse IgG. In both images, cell lysates were immunoprecipitated (+, lanes 1–4) or only lysis buffer was used (–, lane 5). To prepare cell lysates, scFv-P19 was pre-transfected (+, lanes 1 and 2) or not transfected (–, lanes 3 and 4). After 24 h, the cells were inoculated with RABV (+, lanes 1 and 3) or mock-infected (–, lanes 2 and 4). In (A), the bands smaller than 30 kDa appear to be non-specific, because lane 5 (containing only the IP antibody) also has these bands. These non-specific bands might be due to the cross-reactivity of the detection antibody (anti-RABV-P) or the secondary antibody (anti-rabbit IgG) with the IP antibody.

in a merged image (Fig. 3D), indicating that these two molecules colocalized in the cytoplasm. In contrast, in MNA cells pre-transfected with scFv-bat-IgG-pCAG, the change in the fluorescence pattern of scFv was not observed after RABV infection even though the transfection efficiency was much lower than that of scFv-P19-pCAG, and the fluorescence of scFv and RABV-P did not overlap (Fig. 3E–H).

Subsequently, to obtain direct evidence of intracellular binding between scFv-P19 and RABV-P, we immunoprecipitated a lysate of CVS-11-infected MNA cells expressing scFv-P19 with an anti-myc MoAb 48 h after infection. A Western blot analysis using anti-RABV-P polyclonal serum (Fig. 4A) and the anti-myc MoAb (Fig. 4B) showed a 38-kDa RABV-P band (Fig. 4A, lane 1) and a 29-kDa scFv band (Fig. 4B, lane 1), whereas only the scFv band was present in mock-infected cells (Fig. 4B, lane 2). This indicates that these two molecules, scFv-P19 and RABV-P, can associate with each other when co-expressed in the cytoplasm.

Taken together, these results suggest that scFv-P19 is able to recognize and bind to the target protein, RABV-P, intracellularly and to function as an intrabody.

3.4. Inhibition of RABV propagation by the intrabody

Finally, we determined the inhibitory effect of intracellularly expressed scFv-P19 on RABV propagation. MNA cells in 96-well plates were transiently transfected with scFv-P19-pCAG, and 24 h later the cells were infected with CVS-11 at an m.o.i. of 0.005. In this assay, we aimed to observe how the intrabody could inhibit the spread of RABV infection from a limited initial area to simulate the early phase of real viral infection *in vivo*. In order to have the infected area as limited as possible on day 1, we used a low m.o.i. here. We used two separate methods to compare the inhibitory effect of scFv-P19 in scFv-expressing cells and nontransfected cells: measuring the inhibition of the spread of RABV-infected cells in a culture plate (Figs. 5 and 6A), and titration of viruses in the supernatant (Fig. 6B). The data were collected for 4 days after the infection, during which the intracellular expression of scFv-P19 was high and stable (Fig. 5, bottom panel). Cells expressing scFv-P19 substantially inhibited the spread of the RABV-infected area for 4 days (Fig. 5, middle panel), whereas in nontransfected control cells, RABV infection had spread throughout the well within that time (Fig. 5, top panel). The highest inhibitory effect (calculated from the ratio of the proportion of RABV-infected cells in scFv-expressing cells to that in nontransfected cells) was achieved at 3 days after infection ($[1-0.91/66.99] \times 100 = 98.6\%$ inhibition; Fig. 6A). In the experiment involving virus titration, the highest inhibitory effect (calculated from the ratio of the virus titer in

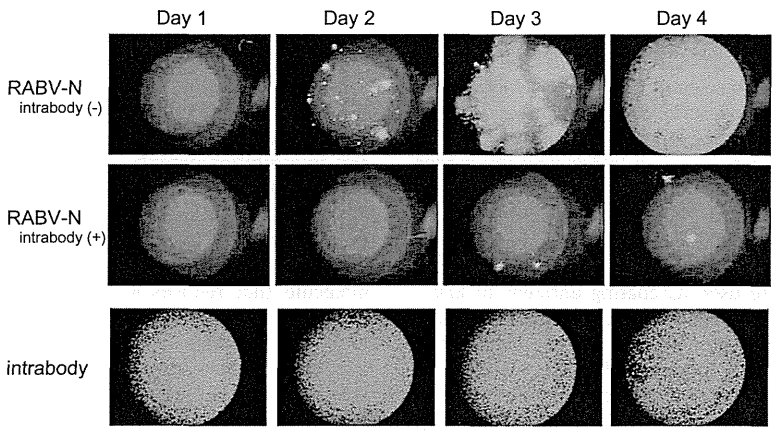

Fig. 5. Comparison of the spread of RABV infection between intrabody-positive and intrabody-negative MNA cells. CVS-11-infected MNA cells without pre-expression of scFv-P19 (top panel), or with pre-expression (middle and bottom panel). The infected cells were stained by FITC Anti-Rabies Monoclonal Globulin on days 1–4 after infection, and the areas that stained positive were compared. In the bottom panels, scFv expression was monitored by staining with a mouse anti-myc tag MoAb and FITC-conjugated anti-mouse IgG; FITC-derived images of scFvs were digitally converted to violet color to avoid confusion with the FITC-derived images of RABV-N in the top and middle panels.

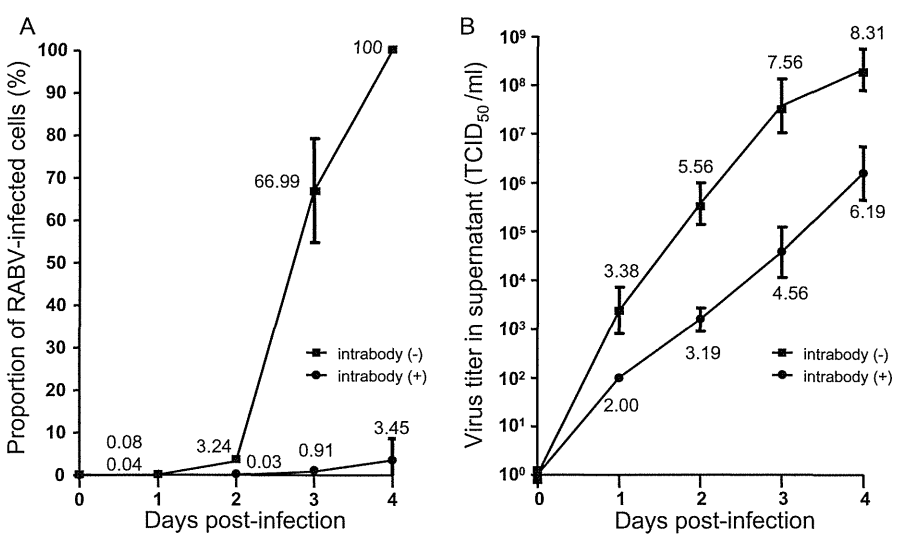

Fig. 6. Inhibition of RABV propagation in MNA cells by intrabody scFv-P19. (A) Time course of the proportion of RABV-infected area relative to the whole well, in a 96-well plate of CVS-11-infected MNA cells without pre-expression of scFv-P19 (■), or with pre-expression of scFv-P19 (●); data were derived from the digitally captured images shown in Fig. 5. Values are mean ± standard error of the mean (SE); $N = 4$. (B) Time course of the virus titer ($TCID_{50}$/ml) in the supernatant of CVS-11-infected MNA cells without pre-expression of scFv-P19 (■), or with pre-expression of scFv-P19 (●). Values are mean ± SE; $N = 4$. The numbers on the graph indicate the logarithm of the mean.

scFv-expressing cells to that in nontransfected cells) was also achieved at 3 days after infection ($[1-10^{4.56}/10^{7.56}] \times 100 = 99.9\%$ inhibition; Fig. 6B)

These results indicate that scFv-P19, when expressed intracellularly as an intrabody, is effective at inhibiting RABV propagation until at least 4 days after infection.

4. Discussion

To our knowledge, this is the first report of intrabody-mediated inhibition of RABV propagation and secretion in studies using mouse neuronal cell lines. A significant reduction in RABV propagation was achieved by pretransfection of an scFv expression vector expressing scFv-P19, which was directed against RABV-P. Another intracellular immunization approach against RABV infection, RNAi-based gene silencing, has also been reported to inhibit RABV propagation (Brandao et al., 2007) and to reduce the replication of the viral genome in mouse neuronal cell lines (Israsena et al., 2009). Also, the intracellular expression of peptides mimicking the N-terminus of RABV-P has been shown to have antiviral activity (Castel et al., 2009). However, no studies of antibody-based intracellular immunization aimed at future therapeutic application have been reported, although several research groups have been developing scFvs or Fabs against RABV proteins for diagnosis or prevention. Intracellular immunization based on scFvs is worthy of investigation because scFvs have several advantages, such as high specificity and long half-lives. Many studies have utilized hybridomas producing MoAbs as a source of scFv; however, phage-display libraries have also been used in recent studies be-

cause they provide benefits such as high diversity in the antigenic repertoire and the ability to rapidly select specific antibodies without animal immunization. In this study, we used human single-fold scFv libraries, Tomlinson I + J, to select scFvs against RABV-P.

One of the obstacles to using scFvs or other antigen-binding molecules as intrabodies is the need to preserve their affinity *in vivo*. Many scFvs have been reported to fold incorrectly *in vivo* and to lose their affinity due to the highly reducing conditions inside cells (Ramm et al., 1999; Wörn and Plückthun, 2001). To minimize this problem, our screening procedure was designed to focus on the selection of scFvs recognizing linear epitopes. Both native and denatured antigens were used as coating antigens in ELISA screening, and only clones showing equivalent reactivity against both were selected. Consequently, all four scFvs obtained in this study reacted with RABV-P in a reducing Western blot analysis, indicating that these clones recognize linear epitopes as expected. Considering the substantial inhibition that scFv-P19 showed against RABV propagation, the strategy of targeting scFv recognizing linear epitopes might be generally useful for future intrabody studies.

We chose RABV-P as the target protein because it contributes to diverse functions through interactions with several viral and cellular proteins. These functions occur at various stages of the RABV life cycle and include encapsidation of viral genome RNA (together with RABV-N and -L), acting as a cofactor for viral RNA polymerase (RABV-L), and inhibiting the interferon-induced cellular antiviral system by binding to signal transducer and activator of transcription 1 (STAT1) and STAT2 to retain them in the cytoplasm (reviewed by Schnell et al., 2010). These multiple functions of RABV-P may be achieved by its efficient modular organization (Gerard et al., 2009) and by the synthesis of four N-terminally truncated P products (P2–P5) showing different subcellular localizations (Blondel et al., 2002): full-length P and P2 are located in the cytoplasm, whereas P3, P4, and P5 are in the nucleus. The detailed three-dimensional structure of P has only been obtained for its C-terminal domain, and how it produces these multiple functions through interactions with various protein counterparts is still not fully understood. The intrabodies against RABV-P obtained in this study were expected to inhibit at least one of these functions, leading to the eradication of viral propagation. Because the epitopes recognized by scFv-P19 (and other clones) have not yet been determined, at the moment there is no evidence regarding which RABV-P function(s) these scFvs block. Our observation that scFv-P19 colocalized with RABV-P in Negri bodies, as well as being diffusely distributed in the cytoplasm, raises the possibility that scFv-P19 inhibits several RABV-P functions in different subcellular locations. Negri bodies, composed of RABV ribonucleoproteins (RABV-N, -P, -L proteins and the RABV genome) and several cellular proteins, are considered to be a marker of RABV infection and are key structures for the synthesis of descendant viral particles (Lahaye et al., 2009). To understand the mechanism through which the scFvs inhibit viral propagation, epitope mapping of the scFvs combined with detailed three-dimensional analysis of RABV-P will be required.

In this study, pretransfection of the scFv-P19 gene into MNA cells substantially inhibited the propagation of RABVs and reduced the virus titer in the supernatant to 1:1000 of that of nontransfected cells at 3 days after infection. This indicates that scFv-P19 could be a prospective candidate for an intrabody; however, this remarkable inhibition might have been achieved partially due to an unexpectedly higher transfection efficiency compared to other scFv clones (scFv-P38, -80, and -115). Although the cause of the difference in transfection efficiency is not clear, a more stable and reliable expression and delivery system should be explored in future studies. One plausible option would be to use a viral vector, which would enable both higher transfection efficiency and strict tropism. These features are especially advantageous for therapeutic application against RABV, which shows extremely high tropism for neuronal cells and propagates by cell-to-cell transmission. By using a viral vector, the other three clones we identified (scFv-P38, -80, and -115), which were not explored further in this study due to low transfection efficiency, might attain higher expression and an inhibition potency as powerful as scFv-P19.

Intrabody research generally consists of two dimensions: the determination of a candidate molecule as an intrabody, and the establishment of an appropriate delivery or application system. This study is the first to report the identification of a candidate molecule that reduces RABV propagation when pretransfected. However, considering the potential of intrabodies as therapeutic tools against RABV infection, post-exposure applications should also be investigated. In this study, we were not able to examine post-exposure application of intrabodies because the high transfection efficiency required for a post-exposure study could not be attained with the transient expression system used. A combination of the scFvs generated in this study and efficient delivery systems involving viral vectors could be powerful tools for future practical studies of post-exposure applications.

In conclusion, we demonstrated that scFv-P19, when pre-expressed as an intrabody in MNA cells, substantially inhibited the propagation of RABV CVS-11. This scFv-based intracellular immunization could be a candidate for a future therapeutic tool against RABV infection if combined with an appropriate delivery and application system, such as a viral vector.

Acknowledgment

This study was supported in part by Health and Labor Sciences Research Grants from Research on International Cooperation in Medical Science. We are grateful to Dr. Mitsuru Sato of the National Institute of Agrobiological Sciences for providing expertise on generating intrabodies.

Appendix A. Supplementary data

Supplementary data associated with this article can be found, in the online version, at doi:10.1016/j.antiviral.2011.04.016.

References

Baltimore, D., 1988. Gene therapy. Intracellular immunization. Nature 335, 395–396.

Blondel, D., Regad, T., Poisson, N., Pavie, B., Harper, F., Pandolfi, P.P., De Thé, H., Chelbi-Alix, M.K., 2002. Rabies virus P and small P products interact directly with PML and reorganize PML nuclear bodies. Oncogene 21, 7957–7970.

Brandao, P.E., Castilho, J.G., Fahl, W., Carnieli, P., Oliveira Rde, N., Macedo, C.I., Carrieri, M.L., Kotait, I., 2007. Short-interfering RNAs as antivirals against rabies. Braz. J. Infect. Dis. 11, 224–225.

Cao, T., Heng, B.C., 2005. Intracellular antibodies (intrabodies) versus RNA interference for therapeutic applications. Ann. Clin. Lab. Sci. 35, 227–229.

Castel, G., Chtéoui, M., Caignard, G., Préhaud, C., Méhouas, S., Réal, E., Jallet, C., Jacob, Y., Ruigrok, R.W.H., Tordo, N., 2009. Peptides that mimic the amino-terminal end of the rabies virus phosphoprotein have antiviral activity. J. Virol. 83, 10808–10820.

Chenik, M., Chebli, K., Gaudin, Y., Blondel, D., 1994. In vivo interaction of rabies virus phosphoprotein (P) and nucleoprotein (N): existence of two N-binding sites on P protein. J. Gen. Virol. 75, 2889–2896.

Chenik, M., Schnell, M., Conzelmann, K.K., Blondel, D., 1998. Mapping the interacting domains between the rabies virus polymerase and phosphoprotein. J. Virol. 72, 1925–1930.

Corte-Real, S., Collins, C., Aires da Silva, F., Simas, J.P., Barbas, C.F., Chang, Y., Moore, P., Goncalves, J., 2005. Intrabodies targeting the Kaposi sarcoma-associated herpesvirus latency antigen inhibit viral persistence in lymphoma cells. Blood 106, 3797–3802.

Dykxhoorn, D.M., Novina, C.D., Sharp, P.A., 2003. Killing the messenger: short RNAs that silence gene expression. Nat. Rev. Mol. Cell Biol. 4, 457–467.

Gerard, F.C.A., Ribeiro, E.D.A., Leyrat, C., Ivanov, I., Blondel, D., Longhi, S., Ruigrok, R.W.H., Jamin, M., 2009. Modular organization of rabies virus phosphoprotein. J. Mol. Biol. 388, 978–996.

Goncalves, J., Silva, F., Freitas-Vieira, A., Santa-Marta, M., Malhó, R., Yang, X., Gabuzda, D., Barbas, C., 2002. Functional neutralization of HIV-1 Vif protein by intracellular immunization inhibits reverse transcription and viral replication. J. Biol. Chem. 277, 32036–32045.

Hemachudha, T., Sunsaneewitayakul, B., Desudchit, T., Suankratay, C., Sittipunt, C., Wacharapluesadee, S., Khawplod, P., Wilde, H., Jackson, A.C., 2006. Failure of therapeutic coma and ketamine for therapy of human rabies. J. Neurovirol. 12, 407–409.

Israsena, N., Supavonwong, P., Ratanasetyuth, N., Khawplod, P., Hemachudha, T., 2009. Inhibition of rabies virus replication by multiple artificial microRNAs. Antiviral Res. 84, 76–83.

Jiang, W., Venugopal, K., Gould, E.A., 1995. Intracellular interference of tick-borne flavivirus infection by using a single-chain antibody fragment delivered by recombinant Sindbis virus. J. Virol. 69, 1044–1049.

Karthe, J., Tessmann, K., Li, J., Machida, R., Daleman, M., Häussinger, D., Heintges, T., 2008. Specific targeting of hepatitis C virus core protein by an intracellular single-chain antibody of human origin. Hepatology 48, 702–712.

Kojima, A., Yasuda, A., Asanuma, H., Ishikawa, T., Takamizawa, A., Yasui, K., Kurata, T., 2003. Stable high-producer cell clone expressing virus-like particles of the Japanese encephalitis virus e protein for a second-generation subunit vaccine. J. Virol. 77, 8745–8755.

Lahaye, X., Vidy, A., Pomier, C., Obiang, L., Harper, F., Gaudin, Y., Blondel, D., 2009. Functional characterization of Negri bodies (NBs) in rabies virus-infected cells: evidence that NBs are sites of viral transcription and replication. J. Virol. 83, 7948–7958.

Marasco, W.A., 1997. Intrabodies: turning the humoral immune system outside in for intracellular immunization. Gene Ther. 4, 11–15.

Motoi, Y., Inoue, S., Hatta, H., Sato, K., Morimoto, K., Yamada, A., 2005. Detection of rabies-specific antigens by egg yolk antibody (IgY) to the recombinant rabies virus proteins produced in *Escherichia coli*. Jpn. J. Infect. Dis. 58, 115–118.

Nawtaisong, P., Keith, J., Fraser, T., Balaraman, V., Kolokoltsov, A., Davey, R.A., Higgs, S., Mohammed, A., Rongsriyam, Y., Komalamisra, N., Fraser, M.J., 2009. Effective suppression of Dengue fever virus in mosquito cell cultures using retroviral transduction of hammerhead ribozymes targeting the viral genome. Virol. J. 6, 73.

Nigg, A.J., Walker, P.L., 2009. Overview, prevention, and treatment of rabies. Pharmacotherapy 29, 1182–1195.

Ramm, K., Gehrig, P., Plückthun, A., 1999. Removal of the conserved disulfide bridges from the scFv fragment of an antibody: effects on folding kinetics and aggregation. J. Mol. Biol. 290, 535–546.

Reed, L., Muench, H., 1938. A simple method of estimating fifty percent endpoints. Am. J. Hyg. 27, 493–497.

Schnell, M.J., McGettigan, J.P., Wirblich, C., Papaneri, A., 2010. The cell biology of rabies virus: using stealth to reach the brain. Nat. Rev. Microbiol. 8, 51–61.

Stein, C.A., Hansen, J.B., Lai, J., Wu, S., Voskresenskiy, A., Høg, A., Worm, J., Hedtjärn, M., Souleimanian, N., Miller, P., Soifer, H.S., Castanotto, D., Benimetskaya, L., Ørum, H., Koch, T., 2010. Efficient gene silencing by delivery of locked nucleic acid antisense oligonucleotides, unassisted by transfection reagents. Nucleic Acids Res. 38, e3.

Vascotto, F., Campagna, M., Visintin, M., Cattaneo, A., Burrone, O.R., 2004. Effects of intrabodies specific for rotavirus NSP5 during the virus replicative cycle. J. Gen. Virol. 85, 3285–3290.

Vidy, A., El Bougrini, J., Chelbi-Alix, M.K., Blondel, D., 2007. The nucleocytoplasmic rabies virus P protein counteracts interferon signaling by inhibiting both nuclear accumulation and DNA binding of STAT1. J. Virol. 81, 4255–4263.

Willoughby, R.E., Tieves, K.S., Hoffman, G.M., Ghanayem, N.S., Amlie-Lefond, C.M., Schwabe, M.J., Chusid, M.J., Rupprecht, C.E., 2005. Survival after treatment of rabies with induction of coma. N. Engl. J. Med. 352, 2508–2514.

Wörn, A., Plückthun, A., 2001. Stability engineering of antibody single-chain Fv fragments. J. Mol. Biol. 305, 989–1010.

Yamamoto, M., Hayashi, N., Takehara, T., Ueda, K., Mita, E., Tatsumi, T., Sasaki, Y., Kasahara, A., Hori, M., 1999. Intracellular single-chain antibody against hepatitis B virus core protein inhibits the replication of hepatitis B virus in cultured cells. Hepatology 30, 300–307.

Jpn. J. Infect. Dis., 64, 391-396, 2011

Original Article

Molecular Epidemiology of Rabies Virus in Vietnam (2006–2009)

Anh K. T. Nguyen*, Dong V. Nguyen, Giang C. Ngo, Thu T. Nguyen, Satoshi Inoue[1], Akio Yamada[1], Xuyen K. Dinh, Dung V. Nguyen[2], Thao X. Phan[2], Bao Q. Pham[3], Hien T. Nguyen, and Hanh T. H. Nguyen

Department of Virology, National Institute of Hygiene and Epidemiology, Hanoi, Vietnam;
[1]Department of Veterinary Science, National Institute of Infectious Diseases, Tokyo 162-8640, Japan;
[2]The Sub-Department of Animal Health of Ho Chi Minh City; and
[3]Center for Preventive Medicine of Gia Lai Province, Vietnam

(Received March 16, 2011. Accepted July 7, 2011)

SUMMARY: This study was aimed at determining the molecular epidemiology of rabies virus (RABV) circulating in Vietnam. Intra vitam samples (saliva and cerebrospinal fluid) were collected from 31 patients who were believed to have rabies and were admitted to hospitals in northern provinces of Vietnam. Brain samples were collected from 176 sick or furious rabid dogs from all over the country. The human and canine samples were subjected to reverse transcription-polymerase chain reaction analysis. The findings showed that 23 patients tested positive for RABV. Interestingly, 5 rabies patients did not have any history of dog or cat bites, but they had an experience of butchering dogs or cats, or consuming their meat. RABV was also detected in 2 of the 100 sick dogs from slaughterhouses. Molecular epidemiological analysis of 27 RABV strains showed that these viruses could be classified into two groups. The RABVs classified into Group 1 were distributed throughout Vietnam and had sequence similarity with the strains from China, Thailand, Malaysia, and the Philippines. However, the RABVs classified into Group 2 were only found in the northern provinces of Vietnam and showed high sequence similarity with the strain from southern China. This finding suggested the recent influx of Group 2 RABVs between Vietnam and China across the border. Although the incidence of rabies due to circulating RABVs in slaughterhouses is less common than that due to dog bite, the national program for rabies control and prevention in Vietnam should include monitoring of the health of dogs meant for human consumption and vaccination for workers at dog slaughterhouses. Further, monitoring of and research on the circulating RABVs in dog markets may help to determine the cause of rabies and control the spread of rabies in slaughterhouses in Vietnam.

INTRODUCTION

Rabies is a fatal zoonotic disease caused by rabies virus (RABV), which belongs to the genus *Lyssavirus* of family *Rhabdoviridae*. Rabies exists in more than 150 countries and territories worldwide. A recent estimate indicates that more than 55,000 people die of rabies every year. However, the actual incidence of human rabies may be 100 times higher than the officially reported numbers, and most of the fatalities due to rabies occur in African and Asian countries (6). In recent years, the number of cases of human rabies in Vietnam, the Philippines, Laos, Indonesia, and China has been rapidly increasing (2,4,8,10,11,13,15). In Vietnam, 362 cases of human rabies have been reported from 2007 to 2010, and the rabies epidemic has occurred in 25–27 provinces (4). The main reservoirs and transmitters of rabies in Vietnam are dogs rather than wild animals such as foxes, bats, and raccoons. Furthermore, most dogs are unvaccinated, and domestic transport and import/export of animals, including dogs and cats, are not well regulated (8). Therefore, determining the genotype of the circulating RABV is very important to understand its evolutionary relationship with the local as well as regional strains and to elucidate the dynamics of the widespread transmission of this disease. The objective of this study was to determine the molecular epidemiology of the RABV circulating in Vietnam.

*Corresponding author: Mailing address: Rabies Laboratory, Virology Department, National Institute of Hygiene and Epidemiology, Hanoi, Vietnam. Tel: +84.4.39724819, Fax: +84.4.39717526, E-mail: nkanhhp@yahoo.com

MATERIALS AND METHODS

Study samples: We collected brain samples from 176 dogs, of which 100 were sick dogs found at slaughterhouses in the northern provinces. These 100 suspected rabies-infected dogs showed at least one of the following signs: refusal to eat or discontinuation of eating, excessive salivation, aggressiveness, and paralyses. The other 76, which were furious rabid dogs, were from the central, highland, and southern provinces in Vietnam. The diagnosis of rabies in those dogs was performed either using fluorescent antibody test (FAT) with the polyclonal antibody raised against the nucleoprotein (N) of RABV (Sanofi Diagnostics, Pasteur, France) or using reverse transcription-polymerase chain reaction (RT-PCR) with a OneStep RT-PCR Kit (Qiagen, Hilden, Germany). Intra vitam samples of saliva (SLV) and cerebrospinal fluid (CSF) were collected from 31 suspected rabies-infected humans who were admitted to national hospitals located in the northern provinces of Vietnam. RT-PCR analysis confirmed that these sam-

ples contained RABV.

Viral RNA extraction and RT-PCR analysis: Total RNA was extracted from 0.3–0.5 g of homogenized brain samples using the RNeasy Mini Kit (Qiagen) and from 0.5 ml of SLV and CSF using the QIAamp Viral RNA Mini Kit (Qiagen). The part of the N gene was then amplified using the QIAGEN OneStep RT-PCR Kit, using a sense primer N7 (nt. 15–34; 5′-ATG TAA CAC CTC TAC AAT GG-3′) and an anti-sense primer JW6E (nt. 601–619; 5′-CAG TTG GCA CAC ATC TTG TG-3′) in a 50-μl reaction mixture containing 400 μM of each dNTP, 10 μl of 5× buffer, 30 μM of each primer, 2 μl enzyme mix, 20 μl distilled water, and 10 μl of the template RNA. The reaction mixture was then subjected to reverse transcription at 50°C for 30 min, followed by heating at 95°C for 15 min, and then 35 cycles of denaturation at 94°C for 1 min, annealing at 54°C for 1 min, and elongation at 72°C for 1.5 min. The mixture was further incubated at 72°C for 15 min to complete elongation. The amplicon was then subjected to electrophoresis in 2% agarose gel and stained with ethidium bromide.

Nucleotide sequencing: The RT-PCR product was excised from the gel and purified using the QIA quick Gel Extraction Kit (Qiagen). Cycle sequencing was performed using N7 and JW6E primers with the ABI 3100 Genetic Analyzer. The nucleotide sequences of the N gene of RABV strains reported in this paper have been submitted to the DDBJ/EMBL/GenBank nucleotide sequence databases (accession numbers AB614372–AB614393 and AB628210–AB628214).

Phylogenetic analysis: The partial nucleotide sequence of N gene (nucleotide position, 85–473) was determined and compared with the representative sequences obtained from the GenBank (www.ncbi.nlm.nih.gov). The accession numbers (the name of strain, country) of the representative sequences are as follows: AB299032 (HCM1, Vietnam); AB299033 (HCM2, Vietnam); AB299034 (HCM5, Vietnam); AB299035 (HCM6, Vietnam); AB299036 (HCM7, Vietnam); AB299037 (HCM8, Vietnam); AB299038 (HCM9, Vietnam); AB299039 (HCM10, Vietnam); AB116579 (VN3, Vietnam); AB116580 (VN52, Vietnam); U22653 (8738THA, Thailand); U22916 (8677MAL, Malaysia); AB070759 (PHI123-01, Philippines); AB 070761 (PHI127-03, Philippines); AB116581 (PHI103, Philippines); AB116582 (PHI114, Philippines); AB070817 (Mdn183/45, Philippines); EF555102 (CQQJDN06, China); EF555106 (SDJNCN01, China); EF555112 (GDZQDN45, China); U22918 (94260NEP, Nepal); EF555098 (CQQJDN02, China); EF555099 (CQQJDN03, China); and EF555100 (CQQJDN04, China). Mokola virus, AY333111 (Eth-16, Ethiopia), was used as an out-group. Complete alignment of nucleotide sequences was performed using ClustalX, version 2.0 (9). MegAlign software version 7.0 (DNASTAR, Madison, Wis., USA) was used to analyze homologies of the nucleotide and deduced amino acid sequences. The neighbor-joining method in MEGA4 version 4.0 (12) was used for constructing the phylogenetic tree with 1,000 bootstrap replications. Epidemiology map was constructed using HealthMapper software, version 4.2, which was supported by the World Health Organization.

RESULTS

Prevalence of rabies in humans and animals: From 2007 to 2009, 31 residents of the northern provinces of Vietnam who were suspected of having rabies were admitted to the Bach Mai Hospital or the Institute for Tropical and Infectious Diseases. We used the CSF and/or SLV samples of these patients for the laboratory diagnosis of rabies. Direct RT-PCR analysis of the patients' SLV and/or CSF samples confirmed that 23 of the 31 (74%) rabies suspected patients were infected with RABV (Table 1). Out of these 23 patients, 12 (52%) had been bitten by dogs or cats and 5 (22%) were involved in the butchering of sick cats or dogs, whereas 6 (26%) did not have any history of dog/cat bites or the butchering of sick animals. In this study, brain samples were collected from 100 sick dogs from slaughterhouses in the northern provinces. The findings of FAT and RT-PCR analysis confirmed that, out of those 100 dogs, 2 (2.0%) were infected with RABV. We also found that 15 (16.4%) of the 76 dogs from the southern and highland provinces were infected with RABV (Table 1).

Phylogenetic analysis: Phylogenetic analysis was performed on 27 strains of RABVs of canine and human origin (Table 2). In the phylogenetic tree, the RABVs

Table 1. Diagnostic results of rabies suspected cases of human and animals (2006–2009)

Location		Human	Animal
Region	Province	Positive/ total (%)	Positive/ total (%)
North	Ha Tay	10/12 (83.3)	2/72 (2.8)
	Hanoi	—	0/4
	Phu Tho	4/4	—
	Bac Ninh	1/1	—
	Hoa Binh	3/3	0/10
	Yen Bai	1/1	—
	Son La	1/1	0/1
	Nghe An	1/1	—
	Lang Son	1/1	0/6
	Tuyen Quang	1/1	—
	Vinh Phuc	0/1	0/1
	Thai Binh	0/1	—
	Unknown	0/1	—
	Ninh Binh	—	0/6
Subtotal	14 provinces	23/28 (82.1)	2/100 (2)
South and Highland	Gia Lai	0/3	3/3
	Lam Dong	—	1/1
	Ho Chi Minh	—	5/53
	Long An	—	1/4
	Soc Trang	—	2/3
	An Giang	—	1/1
	Dong Nai	—	1/4
	Tay Ninh	—	1/1
	Binh Duong	—	0/3
	Tra Vinh	—	0/1
	Tien Giang	—	0/1
	My Tho	—	0/1
Subtotal	12 provinces	0/3 (0)	15/76 (16.4)
Total		23/31 (74.2)	17/176 (9.7)

Table 2. Rabies virus strains used for the phylogenetic analysis isolated from rabies human and dogs, 2006-2009

Case	Location	History	Strain	Year of isolation	Genbank accession no.
Human	Ha Tay	Dog bite	H010607	2007	AB614379
			H040707	2007	AB614380
			H111007	2007	AB614385
			H240808	2008	AB614392
		Dog butchering	H020607	2007	AB628214
			H200608	2008	AB614390
			H280509	2009	AB614393
		Unknown	H140208	2008	AB614387
	Hoa Binh	Dog bite	H230808	2008	—
		Unknown	H170408	2008	AB614389
	Phu Tho	Dog bite	H060907	2007	AB628212
			H071007	2007	AB614382
			H210608	2008	AB614391
		Dog butchering	H091007	2007	AB614384
	Yen Bai	Dog butchering	H050707	2007	AB614381
	Tuyen Quang	Unknown	H150308	2008	AB614388
	Lang Son	Unknown	H130108	2008	AB614386
	Son La	Unknown	H080807	2007	AB614383
Dog	Gia Lai	Aggressive and human attacked	D156	2009	AB628211
			D157	2009	AB614377
			D158	2009	AB614378
	Ho Chi Minh	Aggressive and human attacked	D153	2007	AB614376
			D155	2007	—
	Lam Dong	Aggressive and human attacked	D154	2007	AB628213
	Soc Trang	Aggressive and human attacked	D150	2006	AB614373
	An Giang	Aggressive and human attacked	D151	2006	AB614374
	Long An	Aggressive and human attacked	D152	2007	AB614375
	Ha Tay	Collected from slaughterhouses	D010807	2007	AB614372
			D060807	2007	AB628210

circulating in Vietnam were classified into two major groups: Group 1 consisting of RABVs distributed in the northern, southern, and highland provinces and Group 2 consisting of the strains isolated in the northern provinces (Fig. 1).

Group 1 consisted of RABVs from Thailand, Malaysia, the Philippines, and China, as well as the 11 viruses isolated from humans in the northern provinces and all RABVs from dogs in the highland and southern provinces of Vietnam. Group 1 was further divided into 2 subgroups as shown in Fig. 1. Subgroup 1A consisted of RABVs from Thailand and Malaysia, and all RABVs isolated from dogs located in the southern provinces of Vietnam, and the strains of Ho Chi Minh City, as reported by Yamagata et al. (14). All highland virus strains clustered together (virus strains from D1560609VN to D1580609VN). Subgroup 1B consisted of RABVs from the Philippines and China as well as the 11 RABVs of human origin that were isolated from residents of the northern provinces. Interestingly, the RABV strain H130108VN was clustered with the strain SDJNCN01 from a rabid cow from China. The virus strain H130108VN isolated from a human in Lang Son province located at the Vietnam-China border.

Group 2 consisted of the strains of both human and canine origin isolated in the northern provinces of Vietnam as well as the strains from southern China.

Geographical distribution: The distribution of RABV strains circulating in Vietnam is shown in Fig. 2. The RABV strains in Group 1 were found in 11 of northern, southern, and highland provinces/cities. In contrast, the RABV strains in Group 2 were isolated exclusively in the northern provinces of Vietnam. The circulating of RABV strains belonging to both Group 1 and Group 2 were found in Ha Tay and Phu Tho provinces that experienced a major rabies epidemic (Fig. 2).

DISCUSSION

In Vietnam, the Ministry of Health has devised a system for human rabies surveillance. Thus far, this system has reported the annual data on the number of human deaths due to rabies on the basis of clinical diagnosis alone and not laboratory confirmation. To the best of our knowledge, this is the first report of human rabies confirmed by laboratory diagnosis.

According to the annual reports of the human rabies surveillance program in Vietnam in recent years, human rabies cases have mainly occurred in the northern and highland provinces, particularly in Ha Tay and Phu Tho

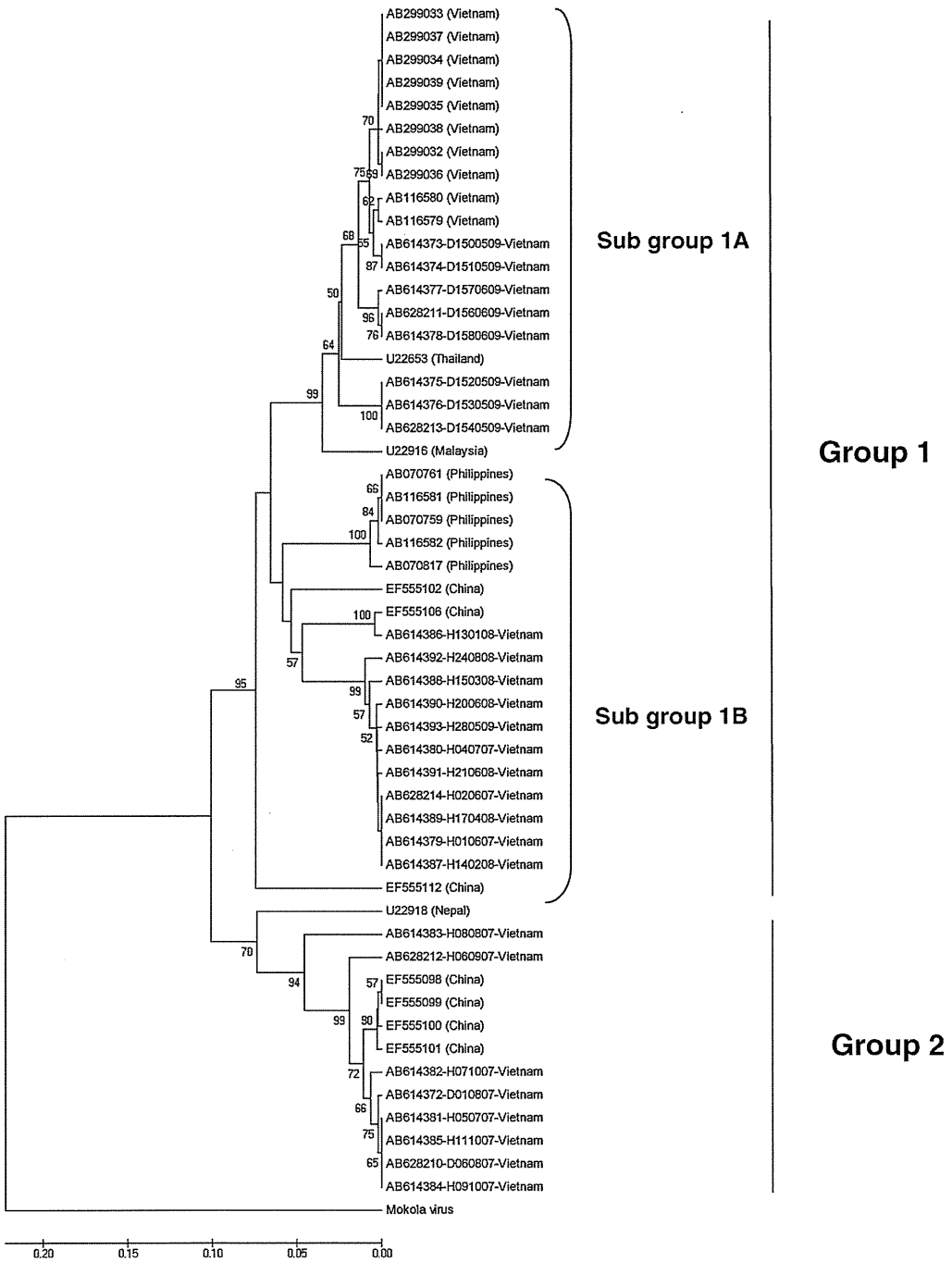

Fig. 1. Neighbor-joining phylogenetic tree based on partial N gene sequences (388 bp) of 27 RABV strains from humans and animals in Vietnam, 2006–2009. Partial nucleotide sequence of N gene (position from 85 to 473) was determined and compared with the representative sequences achieved in the GenBank (www.ncbi.nlm.nih.gov) described as the accession numbers (country). Mokola virus, AY333111 (Eth-16, Ethiopia), was used for an outgroup. Bootstrap values expressed as percentage of 1,000 replicates are shown at tree nodes.

provinces (4). From 2007 to 2009, RABV infection was confirmed in 23 of the 31 rabies suspected patients from 13 provinces. Out of these 23 patients with rabies, 10 were reported in Ha Tay province and 4 were reported in the Phu Tho province. The findings showed that 5 of the 23 rabies patients did not have any history of dog or cat bites, but they had an experience of butchering dogs or cats, or consuming their meat. RABV was detected in 2 of 72 (2.8%) dogs from the slaughterhouses in northern provinces.

Vietnamese communities commonly raise stray dogs, but the dogs are not vaccinated; vaccination coverage is only 10–20% (8). Furthermore, domestic and international transportation of animals is not well regulated in Vietnam. This lack of control has led to the spread of rabies from one region to others, and consequently, to the increase in the number of cases of human rabies. Therefore, strict measures for the control of rabies must

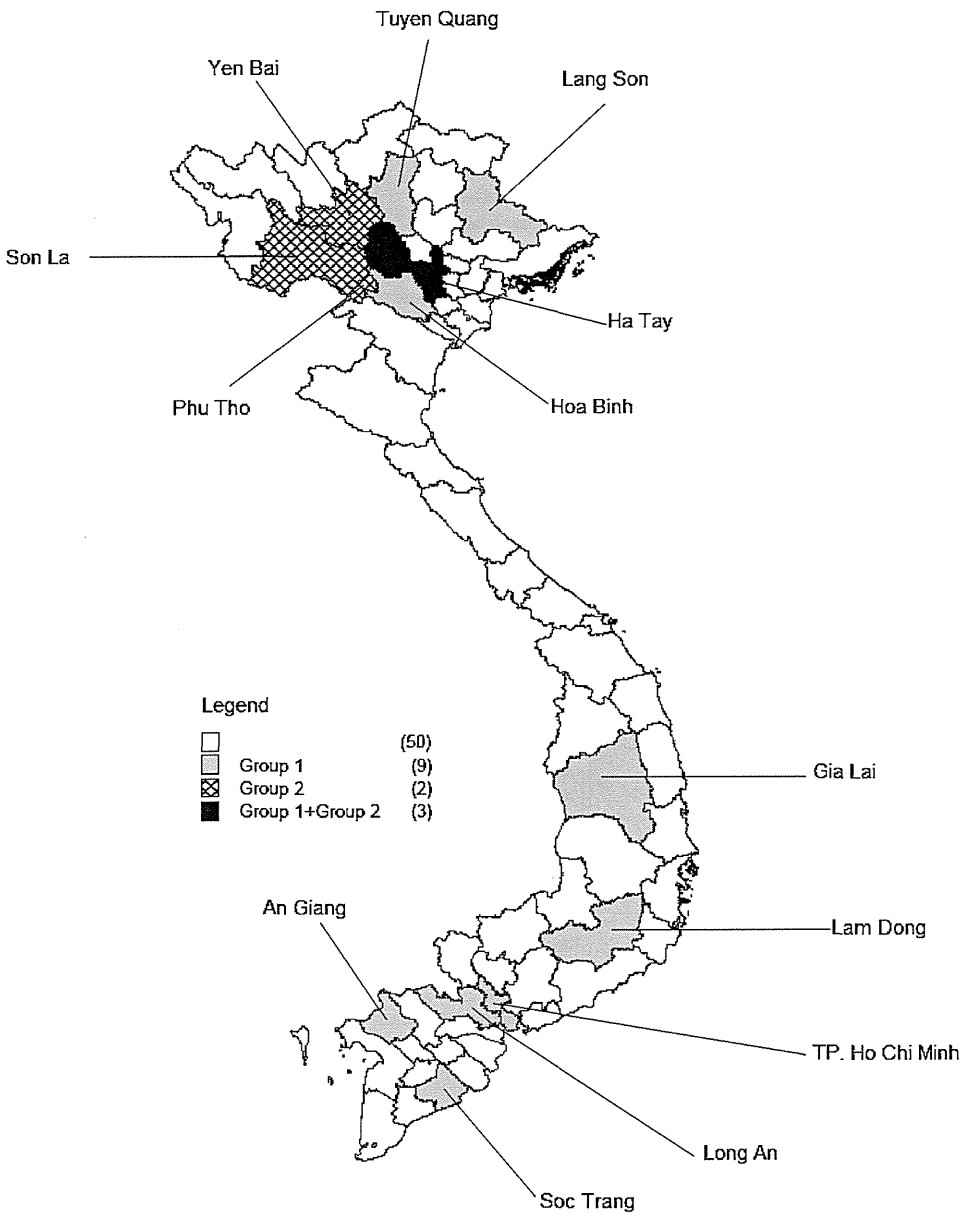

Fig. 2. Topography of RABV strains isolated in Vietnam, 2006–2009. Topographical chart was constructed by HealthMapper software, version 4.2 which is supported by World Health Organization.

be implemented throughout the country. RABV was detected in 2 of the 100 sick dogs (2%) from slaughterhouses located in the northern provinces of Vietnam (Table 1). Previous studies suggest that since some of the infected patients were never bitten by dogs or cats, they must have been infected while butchering the sick dogs or cats (1,3,5,7,15).

The findings of the molecular study showed that at least two different genetic groups of RABV are circulating in Vietnam. Group 1 included strains isolated in Vietnam, and these strains were closely related to those isolated in China, Malaysia, Thailand, and the Philippines. Group 2 consisted of RABVs isolated from humans and dogs in the northern provinces of Vietnam, and these strains were genetically similar to those isolated in southern China (Fig. 1). This finding suggests that the recent increase in cases of infections with Group 2 RABV can be attributable to a constant influx of RABVs from China into Vietnam or vice versa. A previous molecular study conducted by Yamagata et al. (14) in Ho Chi Minh City, Vietnam found that the RABV strains from Vietnam belonged to the South East Asia 1 genotype and were similar to the isolates from Thailand and strain N11 from Guangxi province of China. Further, evidence on the presence of the distinct subgroups in Group 1 (Fig. 1) suggests that RABV may have independently entered Vietnam from several countries such as China, the Philippines, Thailand, and Malaysia and may have established and spread throughout Vietnam.

Strict border control should be implemented to mitigate further influx of RABV from neighboring countries. Although the incidence of rabies due to circulating RABVs in slaughterhouses is less common than

that due to dog bite, the national program for rabies control and prevention in Vietnam should include monitoring of the health of dogs meant for human consumption and vaccination for workers at dog slaughterhouses. Further, monitoring of and research on the circulating RABVs in dog markets may help to determine the cause of rabies and control the spread of rabies in slaughterhouses in Vietnam.

Acknowledgments We would like to thank Dr. Huong Thanh Nguyen (Epidemiology Department, National Institute of Hygiene and Epidemiology, Hanoi, Vietnam) for her help on construction of rabies epidemiology map.

This study was financially supported by the Ministry of Health, Welfare and Labour, Japan and the Ministry of Health, Vietnam.

Conflict of interest None to declare.

REFERENCES

1. Aguilar, E. (2008): Rabies Feared in 30 Dog Meat Eaters. Philippines Daily Inquirer. January 13, 2008.
2. Bounlay Phommasack, et al. (2008): "Country Report on Rabies Control and Prevention in LDR", ASEAN + 3 Conference on Sharing Information on Rabies and Prevention. Halong, Vietnam, April 2008.
3. Wertheim, H.F.L., Nguyen, T.Q., Nguyen, K.A.T., et al. (2009): Furious rabies after an atypical exposure. Plos Med., 6(3), 1-5.
4. Nguyen, H.T. (2009): Rabies in Vietnam. 2nd International Rabies in Asia Conference (RIACON) Proceeding. Hanoi, Vietnam, September 2009.
5. Childs, J.E. (2002): Rabies. Routes of Rabies Virus Transmission to Humans. p. 125-126. Academic Press.
6. Knobel, D., L., Cleaveland, S., Coleman, P.G, et al. (2005): Re-evaluating the burden of rabies in Africa and Asia. Bull. World Health Organ., 83, 1-11.
7. Kureishi, A., Xu, L.Z., Wu, H., et al. (1992): Rabies in China: recommendations for control. Bull. World Health Organ., 70, 443-475.
8. Van, K.D. (2008): "Animals Rabies Control and Prevention in Vietnam", ASEAN + 3 Conference on Sharing Information on Rabies and Prevention. Halong, Vietnam, April 2008.
9. Larkin, M.A., Blackshields, G., Brown, N.P., et al. (2007): Clustal W and Clustal X version 2.0. Bioinformatics, 23, 2947-2948.
10. Deray, R.A. (2008): "Human Rabies in the Philippines", ASEAN + 3 Conference on Sharing Information on Rabies and Prevention. Halong, Vietnam, April 2008.
11. Heng, S. (2008): "Rabies Situation in Cambodia", ASEAN + 3 Conference on Sharing Information on Rabies and Prevention. Halong, Vietnam, April 2008.
12. Tamura, K., Dudley, J., Nei, M. et al. (2007): MEGA4: Molecular Evolutionary Genetics Analysis (MEGA) software version 4.0. Mol. Biol. Evol., 24, 1596-1599.
13. Zhen, X. (2008): "Situation, Surveillance and Control of Rabies in Mainland, China", ASEAN + 3 Conference on Sharing Information on Rabies and Prevention. Halong, Vietnam, April 2008.
14. Yamagata, J., Ahmed, K., Khawplod, P., et al. (2007): Molecular of rabies in Vietnam. Microbiol. Immunol., 51, 833-840.
15. Wallerstein, C. (1999): Rabies cases increase in the Philippines. Br. Med. J., 318, 1306.

Jpn. J. Infect. Dis., 64, 463-472, 2011

Original Article

Gene Expression Analysis of Host Innate Immune Responses in the Central Nervous System following Lethal CVS-11 Infection in Mice

Naoko Sugiura[1,3], Akihiko Uda[1], Satoshi Inoue[1,3]*, Daisuke Kojima[2], Noriko Hamamoto[1,3], Yoshihiro Kaku[1], Akiko Okutani[1], Akira Noguchi[1], Chun-Ho Park[2], and Akio Yamada[1,3]

[1]*Department of Veterinary Science, National Institute of Infectious Diseases, Tokyo 162-8640;*
[2]*Department of Veterinary Pathology, School of Veterinary Medicine, Kitasato University, Aomori 034-8628; and*
[3]*United Graduate School of Veterinary Science, Gifu University, Gifu 501-1193, Japan*

(Received August 12, 2011. Accepted September 9, 2011)

SUMMARY: The central nervous system (CNS) tissue of mice infected with the CVS-11 strain of rabies virus (RABV) was subjected to gene expression analysis using microarray and canonical pathway analyses. Genes associated with innate immunity as well as inflammatory responses were significantly up-regulated, corroborating with the previous findings obtained using attenuated viruses that did not induce a fatal outcome in infected mice. Histopathological examination showed that neurons in the cerebellum had undergone apoptosis. Although the extent of Fas ligand up-regulation was not so prominent, perforin and granzyme genes were highly expressed in the CNS of mice infected with CVS-11. The presence of perforin and granzymes both in the Purkinje cells and CD3 T lymphocytes strongly suggested that apoptosis of the former cells was induced by the latter cells.

INTRODUCTION

Rabies virus (RABV), a member of the genus *Lyssavirus* of the family *Rhabdoviridae*, is known to cause fatal encephalomyelitis in many mammalian species (1). Annually, more than 55,000 individuals die of rabies worldwide. There is often little or no histopathological evidence of neural destruction in animals dying of rabies (2), and the functional changes in RABV infected neurons in vitro are minimal (3). The mechanism underlying RABV infection induced fatal clinical disease and the pathogenesis of rabies are not completely understood.

The neurovirulence of RABV has been mainly studied using animal models that were infected with laboratory strains (fixed virus) having different degrees of pathogenicity. Infection of animals with highly attenuated strains of RABV is not lethal, and profound inflammation accompanied by apoptosis and neural degeneration in the central nervous system (CNS) is noted in such animals. The induction of innate immune responses in the CNS is a hallmark of infection with highly attenuated strains, whereas neural damage is absent or minimal and innate immune responses are not induced in animals infected with street (wild) strains of RABV. A recent study suggested that up-regulation of genes encoding interferon alpha/beta (IFN-α/β) signaling pathways and chemokines was responsible for the elimination of highly attenuated strains from the CNS of infected animals.

Although the challenge virus standard (CVS) strains are a type of fixed RABV, there are several strains of CVS that differ in pathogenicity in different animals. The CVS-24 and CVS-11 have neuroinvasive characteristics and can invade the spinal cord and brain following peripheral inoculation, resulting the death of the infected animals with paralytic symptoms (4–6). In contrast, the CVS-B2c strain, a cloned version of CVS-24, was less pathogenic in adult mice when inoculated intramuscularly. The CVS-F3 strain is apathogenic even in immunocompetent adult mice regardless of the route of infection and causes a transient weight loss in normal mice (7–9).

To precisely understand the mechanisms underlying the pathogenicity of RABV infection, it is crucial to use animal models that most closely reproduce the natural infection. However, conflicting results, in terms of the activation of inflammatory host responses or apoptosis, were sometimes noted even though the same virus strain (CVS-11) was used in these experiments. We hypothesized that these differences were likely caused by a subtle difference in the pathogenicity of respective virus strains used in the experiments.

The aim of this study is to obtain gene expression profiling data from mice infected with pathogenic CVS-11 strain and compare these data with those reported previously in the literature. Although directly comparing the data obtained in different studies is difficult, careful comparison of the data might enable understanding of the possible roles of particular genes involved in the progression of rabies. We expected to elucidate the reason for the conflicting results reported by different studies.

MATERIALS AND METHODS

Cells and virus: Mouse neuroblastoma (MNA) cells were cultivated in minimum essential medium Eagle

*Corresponding author: Mailing address: Department of Veterinary Science, National Institute of Infectious Diseases, 1-23-1 Toyama, Shinjuku-ku, Tokyo 162-8640, Japan. Tel: +81-3-5285-1111, Fax: +81-3-5285-1179, E-mail: sinoue@nih.go.jp

(MEM) (Sigma, St. Louis, Mo., USA) supplemented with 10% heat-inactivated fetal bovine serum (FBS) (Sigma), penicillin (100 U/ml), and streptomycin (100 μg/ml) (Gibco, Invitrogen, Carlsbad, Calif., USA) (MEM-10% FBS). The CVS-11 strain of RABV and MNA cells were kindly provided by Dr. C. E. Rupprecht (Poxvirus and Rabies Branch, DHCPP, NCEZID, CDCP, Atlanta, Ga., USA). The CVS-11 strain was propagated in the MNA cells as described previously (10) and stored at $-80°C$ until use.

Infection of mice with RABV: Six-week-old female C57BL/6J mice were purchased from SLC, Inc., Shizuoka, Japan. Virus suspension (100 μl) containing 10^7 focus-forming units (FFU) of CVS-11 were intramuscularly inoculated into the left hind limb of 18 mice. Twelve mice were inoculated with MEM in a similar way. Mice were humanely sacrificed under anesthesia on days 3 and 7 post-inoculation (pi), and the brains and spinal cords were removed, snap frozen, and kept at $-80°C$. All experiments involving laboratory animals were approved by the institutional animal care and use committee (IACUC) and performed according to the guidelines issued by the IACUC.

Virus titration: Virus titration was performed in quadruplicate, as previously reported (11). In brief, 10-fold dilutions of 10% homogenates of the brains and spinal cords prepared in phosphate buffered saline (PBS(−)) were inoculated onto MNA cells grown in 96-well-plates. After 48 h incubation at 35°C, the cells were washed 3 times with PBS(−) and fixed with 80% acetone for 30 min at room temperature (RT). Next, the infected MNA cells were stained with the fluorescein isothiocyanate (FITC)-conjugated anti-RABV nucleoprotein (N) monoclonal antibody (Fujirebio Diagnostics, Inc., Malvern, Pa., USA) diluted 1:100 in PBS(−) with 0.002% Evans blue for 30 min at RT. The cells were washed 3 times with PBS(−), and the screening for the viral antigen was performed using a UV microscope (Eclipse TE200; Nikon, Tokyo, Japan).

Microarray analysis: Total RNA (300 ng) purified from the brain and spinal cord using RNeasy mini kit (Qiagen, Hilden, Germany) was converted into cDNA using a T7-oligo dT primer. Complementary RNA was transcribed using T7 polymerase in the presence of cyanine-3 (Cy3). Following fragmentation, Cy3-labeled cRNA was hybridized to the Whole Mouse Genome Microarray (44 k probes × 4 arrays/slide) (Agilent, Palo Alto, Calif., USA) at 65°C for 16 h in a rotating hybridization oven at a speed of 10 rounds per min (RPM). Microarray slides were washed sequentially with wash solution 1 (Agilent), wash solution 2 (Agilent), and acetonitrile (Wako, Osaka, Japan). Slides were scanned on an Agilent microarray scanner (Agilent), and the image files were analyzed using feature extraction software (Agilent). Data mining was performed using GeneSpring GX 11 (Agilent). The expression data were normalized with per chip normalization (to the 75th percentile) and per gene normalization (baseline to mean of mock samples). The normalized data were filtered by flags (present or marginal) and fold changes (>2.0). Significant changes in gene expression were found using t test ($P < 0.05$, Benjamini-Hochberg false discovery rate [FDR]). The filtered genes identified by GeneSpring were subjected to further analysis of protein-protein interactions within the context of signaling pathways by Ingenuity Pathway Analysis (IPA) (Ingenuity Systems, Redwood City, Calif., USA).

Quantification of cytokines and chemokines: The levels of cytokines and chemokines were determined by the fluorescent bead immunoassay by Mouse Th1/Th2 10plex FlowCytomix Multiplex (Bender MedSystem, Vienna, Austria) and Mouse Chemokine 6plex FlowCytomix Multiplex kits (Bender MedSystem), according to manufacturer's instructions. Briefly, clarified homogenates prepared from the brains and spinal cords were mixed with beads conjugated with appropriate antibodies, followed by incubation with biotin-conjugated second antibodies and then with phycoerythrin-labeled streptavidin. Washed beads were resuspended in the assay buffer and subjected to flow cytometry on COULTER Epics XL (Beckman Coulter, Fullerton, Calif., USA). BMS FlowCytomix Pro 2.2 software (Bender MedSystem) was used for calculatig the levels of cytokines and chemokines. IFN-β was measured by Mouse IFN-Beta ELISA (PBL Biomedical Laboratories, Piscataway, N.J., USA).

Immunohistochemistry and TUNEL assay: Distribution of RABV antigens as well as the surface markers for neurons and other cellular components in the CNS was determined by immunohistochemistry (IHC) using paraffin-embedded sections, according to the methods reported by Kojima et al. (12). Polyclonal antibody against the phosphoprotein (anti-P antibody) of RABV was obtained by immunization of a rabbit. Anti-glial fibrillary acidic protein (GFAP) (Nichirei Biosciences, Tokyo, Japan), anti-ionized calcium binding adaptor molecule 1 (Iba1) (Wako), anti-CD3 (DAKO, Kyoto, Japan), and anti-CD20 (Spring Bioscience, Fremont, Calif., USA) were used to identify astroglia, microglia, T lymphocytes, and B lymphocytes, respectively. Perforin and granzymes were detected using a rat monoclonal antibody to perforin (Abcam, Cambridge, UK) and biotinylated anti-mouse granzyme B antibody (R&D Systems, Inc, Minneapolis, Minn., USA), respectively. The TUNEL assay was performed as previously described (12,13).

RESULTS

Clinical signs and viral loads: C57BL/6J mice inoculated with CVS-11 showed severe hind limb paralysis on day 7 pi. Of the 9 mice, 4 showed severe paralysis in only 1 hind limb to which the virus was inoculated, whereas the remaining 4 mice showed paralysis of both the hind limbs. Quadriplegia was apparent in 1 mouse. Virus titers in the brains were 1.8×10 FFU/mg on day 3 pi and 2.3×10^5 FFU/mg on day 7 pi, and those in the spinal cords were 6.5×10 FFU/mg on day 3 pi and 5.7×10^3 FFU/mg on day 7 pi.

Microarray analysis: No significant change (fold change >2.0, $P < 0.05$) in the expression level of 41,252 genes in the brains and spinal cords was noted in the mice 3 days after infection with the CVS-11 strain. However, after 7 days of infection, significant changes in gene expression levels were noted in the brains and spinal cords of the infected mice. The results are summarized in a Venn diagram (Fig. 1) by GeneSpring GX 11. Brain specific changes were recognized in the expres-

sion profiles of 1,674 genes, and 1,436 of 1,674 genes were mapped by IPA software using Ingenuity Knowledge Base. Of the 1,436 genes, 780 were up-regulated and 656 were down-regulated by the infection. In the spinal cord, 2,101 genes that showed differential expression were mapped and, of these 640 genes were up-regulated. Interestingly, genes associated with innate immune responses were commonly up-regulated in both the brain and spinal cord (Table 1). Normalization of the data did not affect this propensity, in that, the genes related to innate immune responses, especially those associated with inflammation, such as chemokines, IFNs, and IFN-related genes, were remarkably up-regulated (Table 2). The expression level of IFN-α/β genes was remarkably higher in the brains than in the spinal cords. The gene expression of IFN-β1 and IFN-γ was markedly up-regulated both in the brain and in spinal cord (fold change, 156.5 to 772.3). The levels of genes associated with the activation of IFN signaling pathways were moderately elevated compared to those of IFN-α/β genes. Most genes encoding chemokines were considerably up-regulated. Interleukin (IL) genes and IL-related genes were also up-regulated but to a lesser extent compared to genes encoding chemokines. IL-6 was the only gene that showed high expression level comparable to that of chemokine genes. The expression of CD3 and CD8 genes in the brains and spinal cords showed slight elevation after RABV infection. Expression of genes associated with the elimination of cytotoxic T lymphocytes (CTLs), particularly granzyme genes, was up-regu-

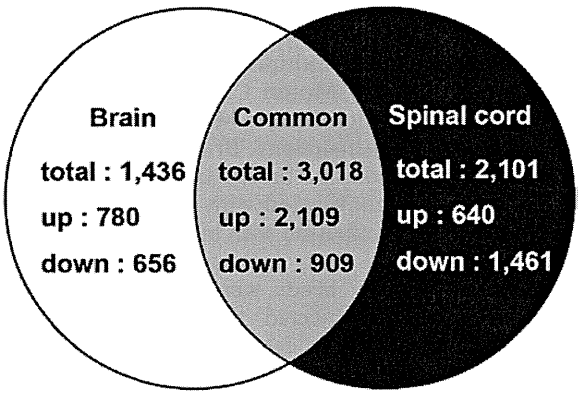

Fig. 1. Venn diagram of up- or down-regulated genes in the brains and the spinal cords after CVS-11 infection. Mice intramuscularly inoculated with 10^7 FFU of CVS-11 into the left hind limb were humanely euthanized on day 7 pi. Mock-infected mice were also sacrificed as controls. RNA ($n = 6$) extracted from the brains and the spinal cords were converted to cDNAs and were subjected to the microarray analysis using Agilent Microarray, feature extraction software and GeneSpring software. The normalized data were filtered by flag and >2-fold changes ($P < 0.05$).

Table 1. Top 10 of biological function categories by IPA

Category	Function Annotation	*P*-value
Common	immune response	6.41E-82
	developmental process of leukocytes	2.20E-62
	developmental process of mononuclear leukocytes	1.38E-58
	developmental process of blood cells	2.23E-58
	activation of leukocytes	4.46E-56
	developmental process of lymphocytes	1.34E-53
	development of leukocytes	7.32E-53
	proliferation of blood cells	1.16E-52
	activation of blood cells	1.66E-52
	quantity of leukocytes	2.46E-52
Brain specific	tumorigenesis	3.30E-11
	cancer	7.19E-09
	tumor	1.19E-08
	neoplasia	1.34E-08
	movement of cells	2.21E-08
	migration of cells	3.05E-08
	migration of eukaryotic cells	1.58E-07
	movement of eukaryotic cells	1.74E-07
	inflammatory disorder	6.13E-07
	cell movement	6.80E-07
Spinal cord specific	coronary artery disease	1.29E-08
	arteriosclerosis	2.77E-08
	atherosclerosis	6.44E-08
	cardiovascular disorder	3.41E-07
	vesicoureteral reflux	5.10E-07
	Dupuytren contracture	1.55E-05
	transport of cation	2.52E-05
	organization of collagen fibrils	2.67E-05
	transport of inorganic cation	6.19E-05
	burn	7.22E-05

Table 2. Expression profile of immunoresponse genes in brains and spinal cords

Gene symbol	Annotation	Probe name	Fold chanage over control	
			Brain	Spinal cord
Interferon				
Ifna1	interferon alpha 1	A_51_P436401	44.0	<2.0
Ifna2	Mouse alpha-interferon (MuIFN-alpha)	A_52_P482280	434.7	13.6
Ifna4	interferon alpha 4	A_51_P355829	323.0	12.7
Ifnb1	interferon beta 1	A_51_P144180	772.3	156.5
Ifng	interferon gamma	A_51_P220976	570.5	525.4
Ifng	interferon gamma	A_52_P68893	517.0	408.6
Ifnar2	interferon (alpha and beta) receptor 2	A_52_P190405	2.6	2.6
Interferon response genes				
Stat1	signal transducer and activator of transcription 1	A_52_P496503	14.3	10.3
Stat1	signal transducer and activator of transcription 1	A_52_P70255	28.6	21.7
Stat1	signal transducer and activator of transcription 1	A_52_P505218	16.8	10.9
Stat1	signal transducer and activator of transcription 1	A_52_P70261	32.2	24.7
Stat2	signal transducer and activator of transcription 2	A_51_P225808	7.1	11.6
Stat3	signal transducer and activator of transcription 3	A_51_P201480	4.9	3.4
Stat3	signal transducer and activator of transcription 3	A_52_P569499	3.1	2.8
Irf1	interferon regulatory factor 1	A_52_P175685	44.3	24.8
Irf1	interferon regulatory factor 1	A_51_P146103	54.8	29.4
Irf2	interferon regulatory factor 2	A_51_P316523	4.4	3.4
Irf5	interferon regulatory factor 5	A_51_P346668	20.4	11.7
Irf7	interferon regulatory factor 7	A_51_P421876	189.5	142.1
Irf8	interferon regulatory factor 8	A_52_P354823	22.2	8.2
Irf8	interferon regulatory factor 8	A_51_P187253	18.8	8.5
Jak2	Janus kinase 2	A_51_P483231	4.1	2.9
Jak2	Janus kinase 2	A_52_P309376	2.4	2.4
Oasla	2′-5′ oligoadenylate synthetase 1A	A_52_P337357	130.5	69.4
Oaslb	2′-5′ oligoadenylate synthetase 1B	A_52_P110877	91.8	43.1
Oaslc	2′-5′ oligoadenylate synthetase 1C	A_51_P428529	6.1	3.6
Oasle	2′-5′ oligoadenylate synthetase 1E	A_51_P134030	4.9	3.5
Oaslf	2′-5′ oligoadenylate synthetase 1F	A_51_P154842	125.2	62.0
Oaslg	2′-5′ oligoadenylate synthetase 1G	A_51_P355267	13.2	13.0
Ifi35	interferon-induced protein 35	A_51_P414889	39.0	24.5
Ifit1	interferon-induced protein with tetratricopeptide repeats 1	A_51_P327751	115.4	72.0
Ifit3	interferon-induced protein with tetratricopeptide repeats 3	A_51_P359570	76.4	85.4
Ifitm1	interferon induced transmembrane protein 1	A_52_P541802	6.5	2.9
Psmb8	proteosome (prosome, macropain) subunit, beta type 8 (large multifunctional peptidase 7)	A_51_P345367	104.4	48.7
Psmb8	proteosome (prosome, macropain) subunit, beta type 8 (large multifunctional peptidase 7)	A_51_P345366	101.9	40.4
Tap1	transporter 1, ATP-binding cassette, sub-family B (MDR/TAP)	A_51_P100327	116.6	63.3
Mx1	myxovirus (influenza virus) resistance 1	A_52_P446431	444.5	268.3
Mx1	myxovirus (influenza virus) resistance 1	A_52_P614259	383.7	235.5
Mx2	myxovirus (influenza virus) resistance 2	A_51_P514085	111.4	47.9
H2-Aa	histocompatibility 2, class II antigen A, alpha	A_52_P343306	1.5	14.5
H2-Ab1	histocompatibility 2, class II antigen A, beta 1	A_51_P215237	1.4	12.4
H2-Ab1	histocompatibility 2, class II antigen A, beta 1	A_52_P570717	1.2	10.3
H2-Ab1	histocompatibility 2, class II antigen A, beta 1	A_51_P215242	1.4	12.9
Chemokine				
Ccl2	chemokine (C-C motif) ligand 2	A_51_P286737	595.4	352.8
Ccl3	chemokine (C-C motif) ligand 3	A_51_P140710	158.8	82.8
Ccl4	chemokine (C-C motif) ligand 4	A_51_P509573	205.7	98.5
Ccl5	chemokine (C-C motif) ligand 5	A_52_P638459	344.1	183.2
Ccl5	chemokine (C-C motif) ligand 5	A_51_P485312	433.5	213.1
Ccl7	chemokine (C-C motif) ligand 7	A_52_P208763	146.4	193.8
Ccl7	chemokine (C-C motif) ligand 7	A_51_P436652	221.2	241.7
Ccl8	chemokine (C-C motif) ligand 8	A_51_P464703	102.1	68.9
Ccl12	chemokine (C-C motif) ligand 12	A_52_P249514	104.5	71.8
Cxcl9	chemokine (C-X-C motif) ligand 9	A_51_P461665	1072.3	289.2
Cxcl10	chemokine (C-X-C motif) ligand 10	A_51_P432641	688.3	358.5

Continued on following page

Table 2—Continued

Gene symbol	Annotation	Probe name	Fold change over control	
			Brain	Spinal cord
Cxcl11	chemokine (C-X-C motif) ligand 11	A_52_P676403	410.2	68.7
Cxcl13	chemokine (C-X-C motif) ligand 13	A_51_P378789	209.8	192.3
Interleukin				
Il1a	interleukin 1 alpha	A_52_P100926	8.4	4.0
Il1a	interleukin 1 alpha	A_51_P438283	6.1	3.2
Il1b	interleukin 1 beta	A_51_P212782	32.9	2.3
Il6	interleukin 6	A_51_P217218	357.2	75.0
Il10	interleukin 10	A_51_P430766	13.5	14.3
Il12b	interleukin 12b	A_51_P385812	59.1	31.4
Tnf	tumor necrosis factor	A_51_P385099	83.4	23.2
IL15 related genes				
Il2ra	interleukin 2 receptor, alpha chain	A_52_P277016	8.5	8.3
Il2ra	interleukin 2 receptor	A_51_P118945	6.9	4.0
Il2rb	interleukin 2 receptor, beta chain	A_51_P286496	29.9	25.2
Il2rg	interleukin 2 receptor, gamma chain	A_51_P456952	22.8	14.1
Il15	interleukin 15	A_52_P15461	5.1	3.8
Il15ra	interleukin 15 receptor, alpha chain	A_51_P202292	6.0	4.2
Il15ra	interleukin 15 receptor, alpha chain	A_52_P55902	5.1	3.5
Cellular activation/Differentiation				
Cd3d	CD3 antigen, delta polypeptide	A_51_P285206	21.2	19.2
Cd3g	CD3 antigen, gamma polypeptide	A_51_P260889	11.6	11.0
Cd8a	CD8 antigen, alpha chain	A_52_P443334	16.8	8.7
Cd8a	CD8 antigen, alpha chain	A_51_P345121	40.4	19.6
Cd8b1	Mouse T-cell membrane glycoprotein (Ly-3)	A_51_P150433	46.2	14.0
Apoptosis related genes				
Casp1	caspase 1	A_51_P142861	11.9	13.0
Casp4	caspase 4	A_51_P511787	112.5	33.6
Casp7	caspase 7	A_51_P414548	6.4	4.2
Casp7	caspase 7	A_52_P260114	7.6	4.4
Casp8	caspase 8	A_51_P247799	11.4	7.5
Fas	Fas (TNF receptor superfamily member)	A_51_P345393	7.4	3.7
Fasl	Fas ligand (TNF superfamily, member 6)	A_52_P77106	14.2	15.2
Fasl	Fas ligand (TNF superfamily, member 6)	A_52_P173985	3.7	5.1
Prf1	perforin 1 (pore forming protein)	A_52_P335178	58.1	61.0
Gzma	granzyme A	A_51_P162794	192.4	96.1
Gzmb	granzyme B	A_51_P333274	546.1	389.6

lated. Canonical pathway analysis indicated that IFN signaling pathway (Fig. 2A) as well as the IL-15 production and signaling pathways was activated (Fig. 2B, 2C). Granzyme B signaling pathway and perforin pathway were also activated in the brains and spinal cords of infected mice (Fig. 2D).

Detection of cytokines: Microarray analysis revealed that RABV infection activated the genes associated with innate immune responses. We, therefore, attempted to determine whether the corresponding proteins were expressed in the brains and spinal cords of infected animals. As shown in Fig. 3A, CCL2, CCL3, CCL5, and CCL7 were highly overexpressed in the brains and spinal cords of infected animals, while CCL4 was expressed only in the brains. The expression of IFN-β and IFN-γ in the brains and spinal cords of infected mice was higher than that in uninfected mice (Fig. 3B). Among the ILs investigated, IL-6 was significantly expressed in the RABV-infected animals. There was a low but significant increase in the production of tumor necrosis factor-alpha (TNF-α), while there was hardly any changes in the expression of other ILs after infection with RABV (Fig. 3C).

Immunohistochemical analysis: Next, we focused on the difference in the expression of some antigens in the infected brains and spinal cords, as revealed by immunohistochemical staining. RABV antigens were hardly detected in the neural cells of the brains and spinal cords 3 days after infection; however, on day 7 pi, viral antigens were widely distributed in the cerebellum as well as in the spinal cords (Fig. 4A). No RABV antigens were detected in mock mice. CD3-positive T lymphocytes and Iba1-positive microglia/macrophages were found in not only the cerebellum but also the spinal cords (Fig. 4B and 4C). However, CD-20-positive B lymphocytes could not be detected. As shown in Fig. 4D, apoptotic neural cells (Purkinje cells) were observed. These Purkinje cells contained cytoplasmic RABV antigens that were detected using anti-P antibody. TUNEL assay also revealed that most T lymphocytes were apoptotic. Cells stained for perforin were detected and scattered in the cerebellar peduncle (Fig.

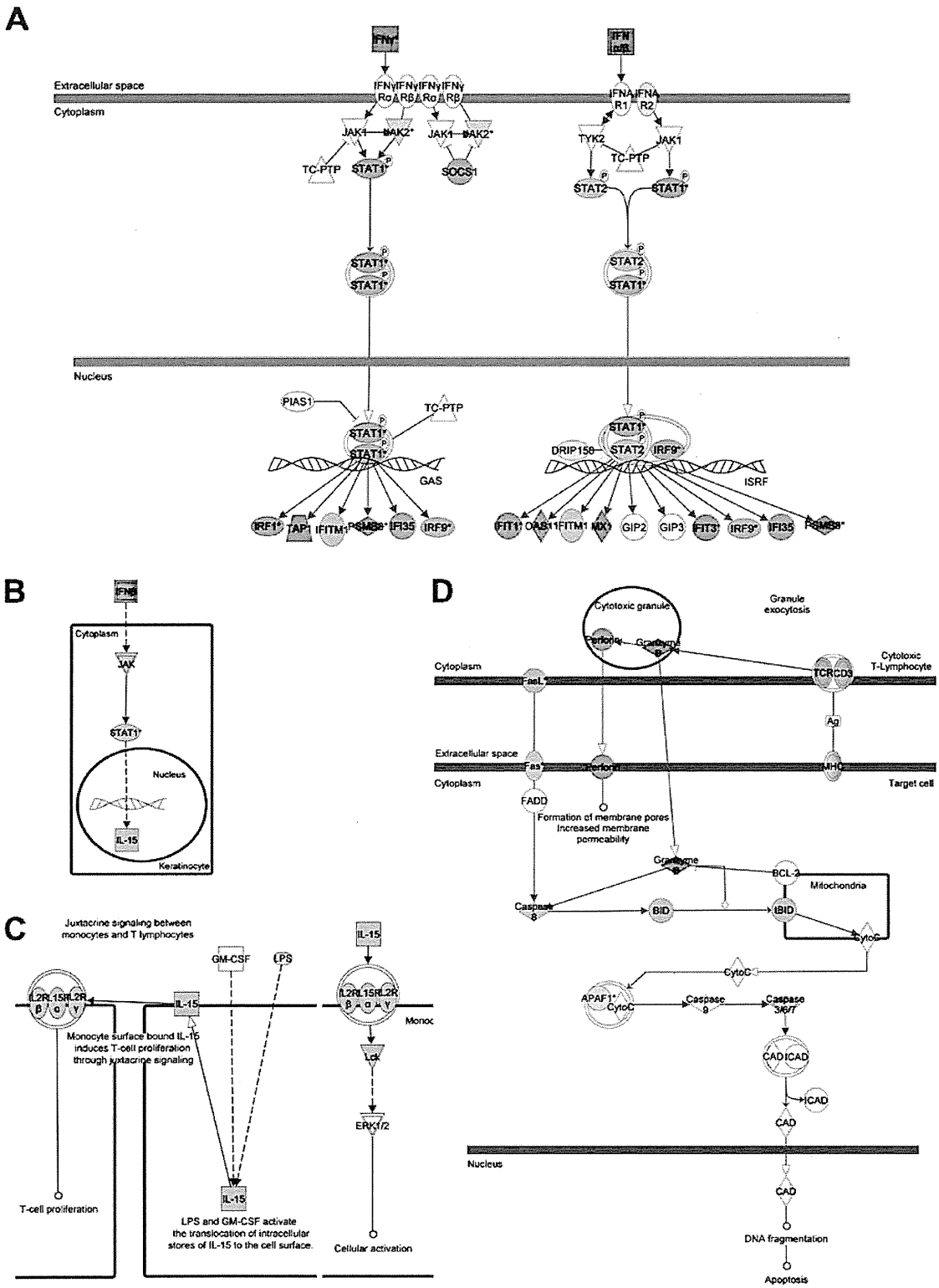

Fig. 2. Pathway analysis of inflammatory responses caused by CVS-11 infection. The genes identified by transcriptome analysis were subjected to Ingenuity Pathway Analysis (IPA). Diagrams show the pathways of interferon signaling (A), IL-15 production (B), IL-15 signaling (C), and Granzyme B signaling (D).

4E) and spinal cords (Fig. 4F). At least 2 cell types, lymphocyte and Purkinje cells, were positive for perforin both in the cerebellum and spinal cords. Granzymes were detected in the Purkinje cells (Fig. 4G) as well as in the infiltrating cells in the spinal cords (Fig. 4H). There was no prominent infiltration of CD3-positive T lymphocytes, increase in Iba1-positive microglia/macrophages, TUNEL-positive neural cells, and cells positive for perforin and granzyme in mock mice.